UiT The Arctic University of Norway

Faculty of Health Science, UiT – The Arctic University of Tromsø

Natural Products and Medicinal Chemistry Research Group, Department of Pharmacy

Clinical Lipidomics: Effects of Vitamin D in Human Adipose Tissue

Sze Mang Sammy Chan

Thesis for the degree Master of pharmacy - May 2021

MASTER THESIS FOR THE DEGREE MASTER OF PHARMACY

Clinical Lipidomics: Effects of Vitamin D in Human Adipose Tissue

By Sze Mang Sammy Chan

SUPERVISORS

Associate Professor Terkel Hansen

Associate Professor Terje Vasskog

Postdoc Yvonne Pasing

PhD Candidate Marita Pérez Syltern

Natural Products and Medicinal Chemistry Research Group

Department of Pharmacy

Faculty of Health Sciences

UiT – The Arctic University of Norway

Acknowledgement

This project was carried out in the period from August 2020 to May 2021 at the Natural Products and Medicinal Chemistry Research Group, Department of Pharmacy, University of Tromsø – The Arctic University of Norway, under the supervision of Associate Professor Terkel Hansen, Associate Professor Terje Vasskog, Postdoc Yvonne Pasing and PhD candidate Marita Pérez Syltern.

First and foremost, I would like to express my sincere gratitude to Terkel Hansen for the invaluable guidance and support throughout this thesis. Thank you for always being available when I needed help or feedback. Your positivity and optimism have been the most encouraging, and I am eternally grateful. I would also like to thank Terje Vasskog for always finding time to help me whenever I ran into problems. I want to thank Yvonne Pasing for the guidance through making sense of the infinite amount of data and turning them into valuable information. I would also like to thank to Marita Pérez Syltern for all the both scientific and non-scientific discussions and the assistance with Compound Discoverer.

I also wish to thank Sietske Grijseels for preparing all of the mobile phases and the help with troubleshooting whenever there is a problem with the orbitrap. My special thanks to my lab mate Torbjørn Norberg Myhre for being the most patient person in the world and helping me through the obstacles of LipidSearch.

I also would like to thank Heba Jawad, for all of our writing sessions and bringing me to all the nice places in Tromsø with good food, and my office mate Sadia Tourè, for all of the long conversations about everything and nothing making this year a lot less lonely and a whole lot more enjoyable.

Finally, I would like to thank my family for always supporting me, encouraging me, and believing in me.

Tromsø, May 2021

Sze Mang Sammy Chan

Table of Contents

List of Tables

List of Figures

Abstract

BACKGROUND: Vitamin D is vital for calcium homeostasis and skeletal health, has immunomodulatory effects and is involved in the regulation of differentiation and proliferation of many different cell types. Adipose tissue is an important metabolic organ and a major organ for vitamin D storage. Although adipose tissue expresses enzymes for vitamin D metabolism and the nuclear vitamin D receptor, the role of vitamin D and its function in adipose tissue is not fully explored.

METHOD: This thesis applies an ether solvent extraction method based on the SIMPLEX method to simultaneously extract lipids and metabolites from 102 adipose tissue samples from a RCT consisting of 51 participants divided to vitamin D (25 participants) or placebo (26 participants) intervention. Extracted lipid samples were analyzed with UHPLC-MS using an AcquireX data acquisition workflow. The lipids were then identified and quantified with LipidSearch. Multivariate data analysis was performed to study the differences between the vitamin D and placebo group. Other analyses, such as pathway analysis, was also performed.

RESULTS: A total of 633 lipid were identified and quantified. No separation was seen in the unsupervised PCA, though applying supervised OPLS demonstrated a separation between supplementation of vitamin D and placebo when using group affiliation as discrimination criterion. Using serum 25(OH)D levels as discrimination criterion showed better separation than when subcutaneous adipose tissue vitamin D levels was used, indicating that lipids in adipose tissue may be affected by vitamin D in other parts of the body than in adipose tissue, e.g. the liver. Out of the 20 most important lipids causing the separation, only 2 were significant ($p \leq 0.05$). 6 out of the 20 contained the fatty acid 4:0 and 4 out of 20 contained either 20:4 or 20:5, possibly indicating vitamin D's activity in production of butyrate and eicosanoid metabolism. Pathway analysis only identified the glycerophospholipid metabolism pathway, though not statistically significant.

CONCLUSION: The results showed a difference in the lipidome between vitamin D and placebo intervention. Though through further examination of the cause of separation, the findings in this thesis were not of statistical significance. Nevertheless, there is much left unexplored and worth further investigation. The metabolite fractions are stored at -80ºC awaiting instrument method development and validation prior to analysis.

List of Abbreviations

Abbreviation	Explanation
1,25(OH)$_2$D	1,25-dihydroxyvitamin D, calcitriol
25(OH)D	25-hydroxyvitamin D, calcidiol
ACN	Acetonitrile
AT	Adipose tissue
BAT	Brown adipose tissue
BMI	Body mass index
DBP	Vitamin D binding protein
DG	Diglyceride
ESI	Electrospray ionization
FA	Formic acid
GPDH	Glycerol-3-phosphate dehydrogenase
HPLC	High performance liquid chromatography
HR-MS	High resolution mass spectrometry
IPA	Isopropanol
LC	Liquid chromatography
LPC	Lysophosphatidylcholine
LPE	Lysophosphatidylethanolamine
MS	Mass spectrometry
MS/MS	Tandem mass spectrometry
MTBE	Methyl-tert-butyl ether
MVA	Multivariate analysis
m/z	Mass/charge
OPLS	Orthogonal partial least squares
PC	Phosphatidylcholine
PCA	Principal component analysis
PE	Phosphatidylethanolamine
PLS	Partial least squares
PS	Phosphatidylserine
QqQ	Triple quadrupole
Q TOF	Quadrupole Time of Flight
ROC	Receiving operating characteristic
RS	Representative sample

RXR	Retinoic acid X receptor
SAT	Subcutaneous adipose tissue
SCFA	Short chain fatty acid
SIMPLEX	Simultaneous Metabolite Protein Lipid Extraction
TG	Triglyceride
UPLC	Ultra-high-performance liquid chromatography
VAT	Visceral adipose tissue
VDR	Vitamin D receptor
VDRE	Vitamin D response elements
WAT	White adipose tissue

1 Introduction

1.1 Background

Vitamin D is not only a vital for calcium homeostasis and skeletal health, but also has immunomodulatory effects in addition to being involved in the regulation of differentiation and proliferation of many different cell types. Adipose tissue is an important metabolic organ with an essential role in energy homeostasis along with being a major organ for vitamin D storage. Although adipose tissue expresses enzymes for vitamin D metabolism and the nuclear vitamin D receptor, the role of vitamin D and its function in adipose tissue is not fully explored. This thesis aims to detect changes in the lipidome in humans occurring upon vitamin D supplementation compared to placebo with the help of lipidomics technologies.

1.2 Vitamin D

Vitamin D is known as the sunshine vitamin. It was first in the industrial revolution in northern Europe that the importance of sunlight for human health was shown. People began gathering in the cities and living in dwelling in close proximity to each other. The atmosphere became polluted as a result of burning of wood and coal. Because of this industrialization children had little direct exposure to sunlight, and as a result developed rickets. Rickets is the failure of mineralization of growing bone and cartilage and was first reported in the 17^{th} century by Daniel Whistler and Francis Glisson in England. In 1822, Sniadecki (1) observed that children in the rural areas outside of Warsaw did not develop the disease. Thus, he hypothesized that rickets was caused by the lack of exposure to direct sunlight in the children residing in the cities, compared to children residing on the farms. In 1890, Palm (2) supported this hypothesis as he observed that children from areas close to the equator were free of this disease despite having poor nutrition. Regardless of Sniadecki's and Palm's observations, by 1900 the disease rickets was so common, the disease became an endemic (3). Eventually, it was discovered that exposure to sunlight and cod liver oil could both prevent and treat rickets. Once vitamin D was identified rickets almost disappeared from industrial countries (4, 5).

1.2.1 Metabolism and Biological Functions

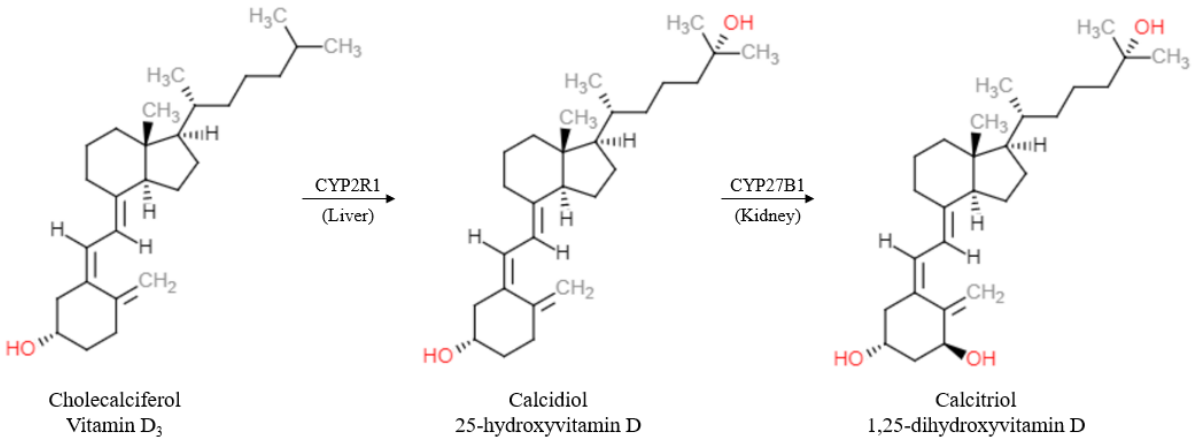

Figure 1-1Structure of vitamin D_3 and its metabolites. Created with ChemDoodle.

Vitamin D is a fat-soluble prohormone normally produced in the skin through ultraviolet irradiation of a derivative of cholesterol, 7-dehydrocholesterol, to produce previtamin D, which then isomerize to vitamin D_3. Vitamin D_3 is a prohormone and the natural form of vitamin D produced in skin, while vitamin D_2 is produced from irradiation of ergosterol (6). The cutaneous production of vitamin D_3 is regulated. At times of prolonged exposure to solar UVB radiation, solar photoproducts inactive on calcium metabolism, such as tachysterol and lumisterol, is produced. This prevents sun induced vitamin D intoxication (7). The production of vitamin D_3 in the skin is influenced by skin pigmentation, use of sunscreen, air pollution, time of the day, altitude, latitude, and season. Because of the increase in the solar zenith angle during winter, early mornings, and late afternoons, the solar UVB photons have a longer travel path through the ozone layer, which absorbs the UVB photons. For this reason, little to no vitamin D is made in skin in winter at above and below approximately 33º latitude. Correspondingly, vitamin D is only synthetized between 10 am and 3 pm at the equator and far southern and northern regions of the world where the sun shines almost 24 hours a day (7). For this reason, the RCT in this thesis is conducted in the winter of Tromsø, where little to no vitamin D is produced in the skin. The enzyme vitamin D 25-hydroxylase (CYP2R1) converts vitamin D into 25-hydroxyvitamin D (25(OH)D), also known as calcidiol, in the liver. The active form of vitamin D, 1,25-dihydroxyvitamin D ($1,25(OH)_2D$) also known as calcitriol, is then generated from 25(OH)D by the enzyme 25-hydroxyvitamin D-1α-hydroxylase (CYP27B1). In the kidneys this activity generates endocrine supply of $1,25(OH)_2D$, while in some extrarenal tissues with CYP27B1 produce $1,25(OH)_2D$ locally for autocrine and paracrine $1,25(OH)_2D$ activity (8).

In the circulation, the majority of vitamin D is bound to vitamin D binding protein (DBP) with high affinity. Vitamin D bound to DBP is transported within the organism, facilitating vitamin D access to various cell types and tissues along with regulating the total amount of vitamin D available for the organism (8). Vitamin D exerts most, if not all, of its physiological effects through its metabolite 1,25(OH)2D. $1,25(OH)_2D$ acts as a nuclear hormone, as it is the only high affinity ligand for the transcription factor vitamin D receptor (VDR) (9). $1,25(OH)_2D$ binds to nuclear VDR, which then binds to retinoic acid X receptor (RXR) to form a heterodimer. The VDR-RXR complex binds to specific nucleotide sequences in the DNA known as vitamin D response elements (VDRE). As a result, the gene's activity can be either up- or down-regulated (7). VDR is expressed in the majority of human tissues and cell types (9).

Vitamin D, in its active form, is essential for intestinal calcium absorption and plays a central role in maintaining calcium homeostasis, phosphorus homeostasis and skeletal integrity. In addition to this $1,25(OH)_2D$ also regulates cell proliferation and differentiation, cellular growth and hormone secretion (10, 11).

Once $1,25(OH)_2D$ is formed it enters the circulation and travels to the small intestine and bone, the principal calcium-regulating target tissues. $1,25(OH)_2D$ binds VDR in the small intestine and activate vitamin D responsive genes to enhance intestinal calcium and phosphorous absorption. However, when dietary calcium is insufficient $1,25(OH)_2D$ travels to the bone and interact with osteoblast, which stimulate the formation of osteoclasts. This results in increased osteoclastic activity, which removes the calcium stores from the bone and deposits it into the blood to maintain calcium homeostasis (7, 12). In a vitamin D deficient state there is a decrease of the intestinal calcium absorption and the total maximal reabsorption of phosphate. Low ionized calcium levels stimulate the secretion of parathyroid hormone (PTH), which increases the tubular reabsorption of calcium in the kidneys and increases CYP27B1 activity and causes increased $1,25(OH)_2D$ synthesis (11). Secondary hyperparathyroidism also results in PTH-induced loss of phosphorous into the urine and decreased phosphorus absorption in the intestines. This leads to low fasting serum phosphorous concentrations. Together with low serum calcium concentration it often results in an insufficient calcium-phosphate product. Calcium-phosphate product is important for the mineralization process. In insufficient conditions, it causes mineralization defects which results in rickets in children and osteomalacia in adults (3).

As VDR is expressed in majority of human tissues and cell types, including heart, stomach, pancreas, brain, skin, gonad, prostate, breast and activated T- and B-lymphocytes, vitamin D also has a multitude of noncalcemic functions (11, 13). Thus, vitamin D has been associated with reducing the risk of many types of cancer, diabetes mellitus, cardiovascular disorders and other illnesses (7).

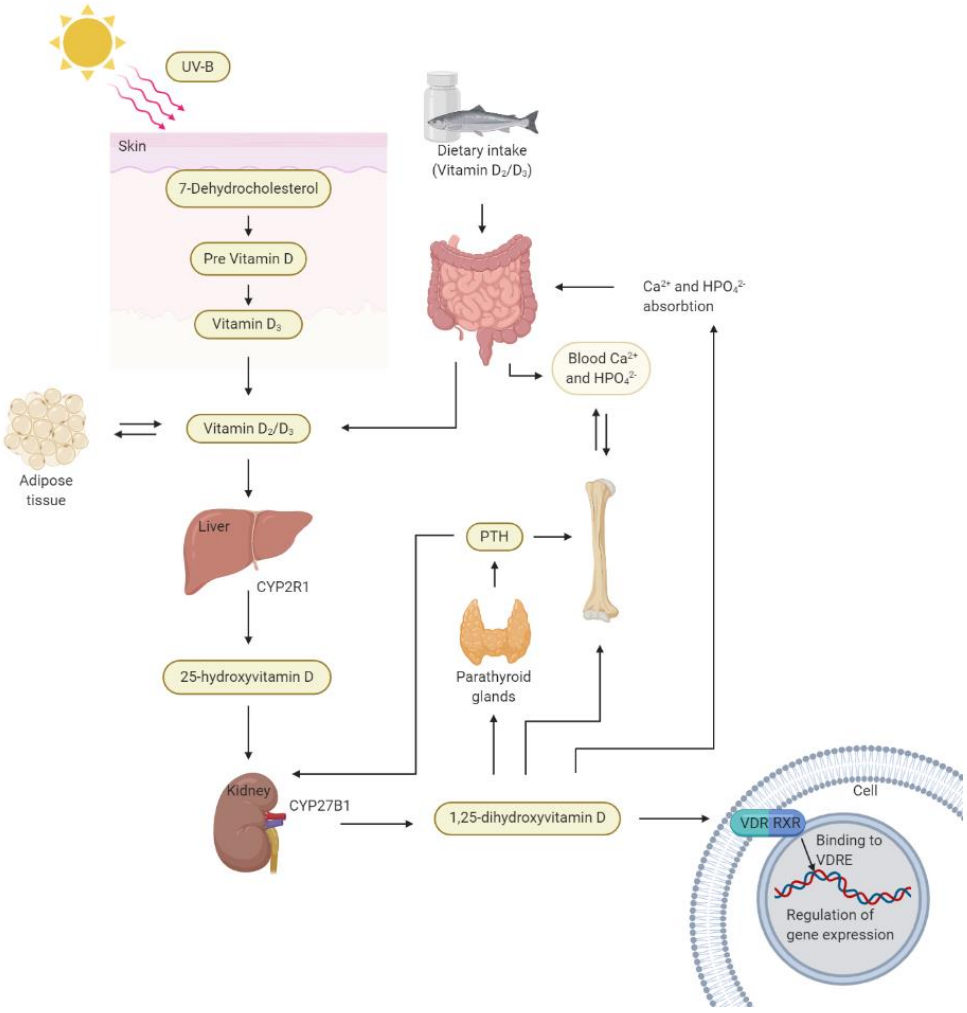

Figure 1-2 Metabolism and biological functions of vitamin D. Created with BioRender.com

1.2.2 Vitamin D Status, Sources and Supplementation Recommendation

Vitamin D is a micronutrient which is needed for optimal health throughout the whole life (14). If vitamin D synthetized in the human skin upon exposure to UV light is insufficient, intake of adequate vitamin D from diet or dietary supplements is essential (14). Vitamin D is found naturally only in very few foods. Fatty fish, such as salmon, mackerel and sardines, and fish liver oils, such as cod liver oil, are good sources of vitamin D, as well as wild mushrooms or sundried mushrooms. The amount of vitamin D in eggs are highly variable, and because of the

cholesterol content eggs are a poor source for vitamin D. Unless fortified, milk contains very little to no vitamin D content, while dairy products, like butter and cheese, shows higher vitamin D content though the amount is still low in a serving size (3, 14).

There is a consensus that 25(OH)D is to be used as an assessment of vitamin D status as 25(OH)D reflects dietary supply and the dermal production, though other novel markers has been investigated and shown to be worthy of further investigation (10). Optimal serum concentrations of 25(OH)D is most commonly defined as the concentration that maximally suppresses serum PTH. Estimates of optimal 25(OH)D concentrations reached with this criterion vary widely from 20 to 110 nmol/L, and no consensus has been reached. In a review, optimal 25(OH)D concentrations were estimated for multiple health outcomes, including bone mineral density and fracture risk reduction, dental health, lower-extremity function, and colorectal cancer prevention. Data in this review suggested that the most advantageous target concentration is 75 nmol/L and optimal concentration is between 90 and 100 nmol/L (15). Institute of Medicine states that serum concentrations below 30 nmol/L is associated with the risk of negative effects on bone health while serum concentrations above 50 nmol/L is sufficient for 97.5% of the population (16). According to the Norwegian guidelines, serum 25(OH)D concentrations between 25-50 nmol/L is considered suboptimal, while 12.5-25 nmol/L is considered deficiency. Similarly, vitamin D levels below 12.5 nmol/L is considered as a severe deficiency. Thus, the general aim is to achieve 25(OH)D concentrations above 50 nmol/L which is considered sufficient (17). The RCT in this thesis includes participants with 25(OH)D concentration in the rang 25-45 nmol/L, which is in the range considered suboptimal.

Table 1-1 Reference values for vitamin D status

Serum 25(OH)D	**Vitamin D status**
>50 nmol/L	Sufficient
25-50 nmol/L	Suboptimal
12.5-25 nmol/L	Deficiency
<12.5 nmol/L	Severe deficiency

To reach the level of vitamin D sufficiency, Institute of Medicine recommend a dietary vitamin D intake of 600 IU/day (15 µg/day) from 1-70 years of age, including pregnant and lactating women, and thereafter 800 IU/day (20 µg/day) (16). The Norwegian Directorate of Health

recommends a dietary intake of 400 IU/day (10 µg/day) between the age of 1-74 years, and 800 IU/day (20 µg/day) for those who has passed the age of 74 years (18).

1.3 Adipose Tissue

The adipose tissue (AT) was previously considered as a simple storage site, but it is now recognized as an important metabolic organ and has an essential role in energy homeostasis (19). AT in humans consist of two major types, white adipose tissue (WAT) and brown adipose tissue (BAT). WAT is made up of subcutaneous WAT (SAT) and visceral WAT (VAT) around internal organs. BAT participates in non-shivering thermogenesis through lipid oxidation, while WAT functions primarily as insulation and energy storage (20). WAT has a limitless capacity for triglyceride storage vital for survival. During a meal, the rise in insulin, glucose and lipids stimulates triglyceride formation and storage in WAT and liver. Opposite, when there is a fall of insulin during fasting glycogen breakdown and lipolysis is triggered through activation of the nervous system and elevation of glucagon, glucocorticoids and epinephrine (19).

Adipocytes has shown to secrete cytokines, hormones, and peptides, collectively termed adipokines. One of the most well studied adipokines is leptin. Leptin inhibits appetite and stimulate satiety by regulating neural circuits in the brain and is secreted in response to food intake. Circulating leptin is elevated in obesity, but because of hypothalamic leptin resistance obesity is aggravated, by inhibiting appetite control and lipid oxidation. Another adipokine is adiponectin. Adiponectin stimulates lipid oxidation and anti-inflammatory responses and through this exerts antidiabetic effects, anti-obesity and alleviates insulin resistance (20).

1.3.1 Vitamin D in Adipose Tissue

AT is the main storage site of vitamin D and expresses VDR and enzymes involved in vitamin D metabolism. In addition, it has been shown that vitamin D regulates adipogenesis as well as adipocyte apoptosis (21).

AT was discovered to be a principle storage site using radiolabeled vitamin D given to vitamin D-deficient weanling rats orally. It was shown that within 24 hours of administration, a significant amount of radioactivity was present in the AT. The release of vitamin D from the AT of the rats was very slow after the vitamin D treatment ceased. After 6 weeks of the vitamin D administration, 80% of all detected radioactivity was present in AT. As the amount of vitamin

D released was proportional to the concentration of vitamin D present in AT, AT shows indications that it has the characteristics of a depot for the storage of vitamin D as well as the release (22). In a more recent human study, it has been demonstrated that a considerable amount of vitamin D is stored in SAT. After 3-5 years of supplementation of 20 000 IU vitamin D per week, vitamin D content in SAT increased by approximately 6-fold compared to placebo (23).

Adiposity is a serious public health problem associated with vitamin D insufficiency due to the decreased bioavailability of vitamin D because of its deposition in body fat compartments. BMI is inversely related to serum 25(OH)D, but there is no evidence for a BMI lowering effect by a higher 25(OH)D (24). Present data suggests that, in obese subjects, the vitamin D system is altered. This may have consequences for the development of obesity and its co-morbidities. The expansion of adipose tissue in obesity is associated with an increase in the accumulation of macrophages in the tissue. Since macrophages are known to hydroxylate 25(OH)D to $1,25(OH)_2D$, this may facilitate the local conversion of 25(OH)D (25).

It has been reported that CYP27B1 is expressed in mouse 3T3-L1 preadipocytes and in adipose tissue of Wistar rats. It is also shown to be expressed by Simpson-Golabii-Beymel syndrome human adipocytes and preadipocytes as well as human mammary adipocytes. Therefore, adipocytes could be involved in local synthesis and degradation of vitamin D. Human mammary adipocytes demonstrated bioactivation of 25(OH)D to $1,25(OH)_2D$, together with the release of $1,25(OH)_2D$ (25).

1.4 Omics

The addition of the suffix “omics” to a molecular term implies a comprehensive, or global, assessment of a set of molecules (26). Omics technology includes genomics, transcriptomics, proteomics, and metabolomics, and are high-throughput technologies that substantially increase the number of genes/proteins/metabolites that can be detected simultaneously. With the use of omics technologies there is a potential to relate complex mixtures to complex effects through gene/protein/metabolites quantification profiles. The primary aim of omics is the nontargeted quantification of all gene products in a biological sample, namely transcripts, proteins and metabolites (27).

1.4.1 Metabolomics

Metabolomics is the study of the metabolome, commonly defined as the complete collection of metabolites, small molecules (<1 500 Da), found in an organism, biofluid, organ, cell, or organelle. In other words, metabolites can consist of many endogenous compounds such as lipids, carbohydrates, short peptides, amino acids, nucleic acids and others, that are produced endogenously during catabolism and anabolism, as well as exogenous compounds (28, 29).

Metabolomics has, historically, been primarily used to diagnose diseases or detect pathological conditions, most likely since metabolomics has been considered as an extension of clinical chemistry. Though, while clinical chemistry typically focuses on one or two compounds at a time, metabolomics looks at hundreds at a time. Because of the metabolomics ability to measure large numbers of varying metabolites, it has become particularly attractive to studying and diagnosing metabolic diseases (28).

1.4.2 Lipidomics

Lipidomics is the science of the large-scale determination of individual lipid species (30), and belong to the last step of the "omic" cascade, the metabolomics. The metabolome represents the qualitative and quantitative information on all metabolites occurring in a biological system, reporting the actual state of the organism. Therefore, it is most convenient for biomarker discoveries of pathological states of an organism (31). Different techniques can be used for metabolomics/lipidomics, such as nuclear magnetic resonance spectroscopy (NMR) or UV, but UPLC-MS provides more identifications and better quantitation with the exception of target analysis (30).

Lipids are a heterogeneous pool of compounds that contain either fatty alkyl, fatty acyl, sphingosine, or isoprene moieties as their hydrophobic building blocks. The lipids are generally classified into eight categories: fatty acyls, glycerolipids, glycerophospholipids, sphingolipids, sterols, prenol lipids, saccharolipids and polyketides. Each of these categories consists of further lipid classes and subclasses (30). This leads to a total of 45 144 lipids in the LIPID MAPS Structure Database (LMSD). Among these 23 191 of the compounds are curated and the remaining 21 953 are computationally generated lipids (November 2020) (32). Thus, lipidomics is challenging as the lipidome comprises thousands of different molecular species highly diverse in chemical structure and composition as well the occurrence of molecular species as isomers or isobars (33).

1.5 Sample Preparation

Appropriate sample preparation is an essential aspect of quantitative bioanalysis. In the sample preparation interfering matrix compounds should be removed to avoid clogging and soiling the instrument, in addition to improving the sensitivity, selectivity and reliability of analyses. Factors such as the analytes characteristics, their expected concentration, sample size and matrix, as well as the availability of analytical techniques are important when selecting an appropriate sample preparation method. Commonly applied sample preparation techniques include protein precipitation, solid-phase extraction, and liquid-liquid extraction (34).

Liquid-liquid extraction is a separation process consisting of the transfer of the solute from one solvent to the another. The two solvents used are immiscible or partially miscible with each other, with one of the solvents usually being water or an aqueous mixture and the other a non-polar organic liquid. Liquid-liquid extraction, like all extraction processes, consists of two steps, mixing followed by phase separation. Both steps are important to consider when selecting solvents and modes of operation (35). Liquid-liquid extraction is in general simpler and less time consuming compared to the other extraction methods and may be applicable to almost all laboratories using large variety of available solvents. It is also less expensive as well as more flexible as several samples may be prepared in parallels. But large volumes of flammable and/or toxic solvents, mutual solubility of analytes in both phases, as well as emulsion formation should be taken into consideration (34).

1.6 High-Performance Liquid Chromatography and Ultra-High-Performance Liquid Chromatography

Chromatography is a term for several similar techniques that separates different molecular species in a mixture, based on differences in rates of migration when the sample components are transported through a stationary phase by a mobile phase. In high-performance liquid chromatography (HPLC) the sample is introduced to a flowing liquid mobile phase that passes a stationary phase, which is typically in the form of a column packed with very small porous particles. The mobile phase is moved through the stationary phase by a pump (36, 37).

A sample is made up of analytes, the molecules of interest, and matrix, the rest of the components. The sample is injected into the mobile phase as a small volume just before the column inlet. The substances to be separated must be dissolved in a liquid that is miscible with

the mobile phase, but not stronger eluting. Difference in migration of the components in the sample depends on the equilibrium distribution of each component between the stationary phase and the mobile phase. The more time a component spends in the stationary phase, the longer the retention and opposite. Therefore, the migration is determined by the composition of the mobile phase, the composition of the stationary phase and the temperature. Detectors provide an electronic response to the analytes when they elute, which is then processed by a computer system that prints the results as chromatograms (36, 37).

Ultra-high-performance liquid chromatography (UPLC) is similar to HPLC, the difference is in the size and shape of the silica particles. In HPLC the size of the particles in the column is usually 3-10 µm, while in UPLC the diameter can be below 2.5 µm. The columns in UPLC is also often shorter in length due to the higher separation performance of the smaller particles. The very small particles also require a significantly higher operation pressure for the mobile phase. UPLC methods are used increasingly due to better and faster separation, major savings in the consumption of mobile phase and lower detection limits (36, 37).

Reversed phase HPLC is the most common HPLC technique. In reversed phase chromatography the stationary phase is hydrophobic, and the mobile phase is a polar aqueous solution. The stationary phases for reversed phase are typically made of silica derivatized with reagents to form a hydrophobic surface, typically by binding hydrophobic groups to the silanol groups, for example long hydrocarbon chains such as C18. The main separation mechanism in reversed phase chromatography is hydrophobic interaction. Therefore, the nonpolar analytes are retained strongly, while polar analytes elute earlier. The main forces of interaction are van der Waal's forces. Van der Waal's forces are relative weak forces, but they are present in a large number per molecule. Thus, the interaction increases with the molecular size. The mobile phases consist of mixtures of water and one or more organic solvents which must be miscible with water. The organic solvents modify the strength of the mobile phase. The strength of the mobile phase increases with the increase of the organic solvents, and the retention of the analytes decrease. Small amounts of buffers can also be added to control the pH and counter ions of ionized groups (36, 37).

1.7 Mass Spectrometry

Mass spectrometry (MS) is performed by using an instrument called mass spectrometer and measures mass over charge (m/z) of atoms, molecules, or fragments of molecules. A mass spectrometer is built from three components, an ion source, a mass analyzer, and a detector. In the ion source, the analyte molecules are ionized to molecular ions or pseudo molecular ions. The mass analyzer then separates the ions according to their m/z. Finally, the abundance of each ion, with a different m/z value, is registered and measured by the detector. The detector is connected to a computer which displays the result as a mass spectrum. MS coupled to liquid chromatography (LC) is abbreviated to LC-MS. A major advantage of coupling MS to LC is the ability to distinguish different substances with similar retention times, as well as separating different compounds with exact same m/z value (36).

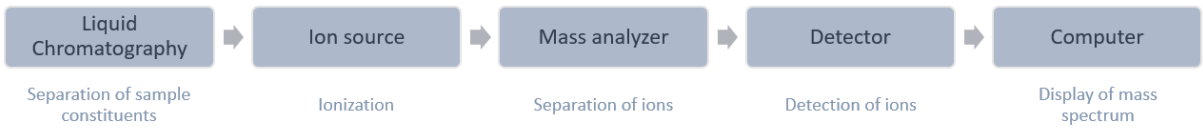

Figure 1-3 Schematic view of LC-MS.

1.7.1 Electrospray Ionization

In the electrospray ionization (ESI) interface, the sample constituents are delivered in a volatile mobile phase from the LC system and passes through a narrow capillary producing a fine aerosol by nitrogen gas flowing along the capillary. An electrode is placed in continuation of the capillary, coupling an electrical potential between the capillary tip and electrode. This transfers the electrical potential to the small drops in the aerosol, resulting in a fine aerosol of charged droplets. The liquid droplets evaporate and are flushed away by a drying gas. When the solvent evaporates of the droplets there are two forces becoming dominant, surface tension in the droplets acting to retain the shape and Coulomb force of repulsion between like charges acting to break down the shape of the droplet. As the solvent evaporates the droplet size decreases and at one point the Coulomb force of repulsion overcome the surface tension and a Coulomb explosion occurs. The droplets disintegrate into much smaller droplets, and the cycle repeats until all of the solvent has been evaporated. The analyte molecules remain charged and are led by electric potential difference into the MS for further analysis (36).

1.7.2 Orbitrap

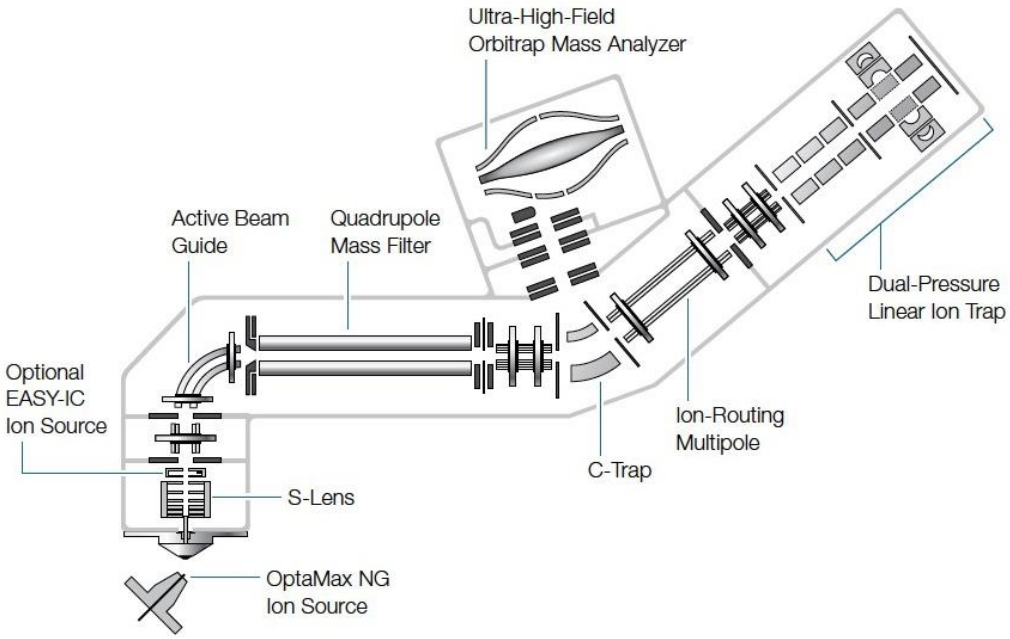

Figure 1-4 Schematic for Orbitrap ID-X MS.

Metabolomics and lipidomics methods require the analysis of complex mixtures, detection of analytes of different types and over a wide range of concentrations. Consequently, there is a need for instruments with better resolution, mass accuracy and tandem mass spectrometry (MS/MS) capabilities. For identification, the use of high-resolution MS (HR-MS) provides accurate mass determinations with four or five decimals. HR-MS can determine the elemental composition of both molecular ions and fragment ions by combining accurate mass determination with search in different data bases, suggestions for elemental composition, structure formulas and in some cases fragmentation patterns when available (36).

The Orbitrap is the youngest member of the family of mass spectrometers. The Orbitrap mass analyzer consists of a solid, spindle-like central electrode that is placed within an outer barrel-like electrode and is a few centimeters in length. In the space between the two electrodes, trapped ions undergo complex oscillations and high-resolution measurements take place. Due to the unique geometric shape of the electrodes, the ions not only rotate at a given orbit around the central electrode, but also produce an axial oscillation along the length of the electrode. The axial oscillation frequency depends entirely on the mass/charge (m/z) ratio of the ion. The orbitrap measures the frequency and the intensity of the oscillating ions. The Orbitraps mass resolving power is directly proportional to the measurement time, as it may take thousands of oscillations until two ions with only slightly different m/z are physically separated. Thus, higher

resolving power comes at the price of longer measurement times. This also results in fewer available datapoints across a chromatographic peak (38).

The ability of the C-trap in the Orbitrap to accumulate ions is one relevant difference that separates the Orbitrap from the conventional triple quadrupole (QqQ) and time of flight (Q-TOF) instruments. The Orbitrap mass analyzer must maintain a low-pressure environment to minimize the collision of oscillating ions with residual gas molecules as much as possible. As the ions have to be accelerated from a high-pressure area to a low-pressure area, the fast injection of a very dense ion cloud is required. The C-trap is able to collect and store ions, and also accelerating the ions into the mass analyzer through a small opening. In addition to this, the increase of the voltage of the central electrode to bend the ion trajectories is essential to enable successful trapping of the ions in the mass analyzer (38).

The fragmentation in the Orbitrap can be done in the high energy collision dissociation (HCD) cell or by collision induced dissociation in the CID cell. Fragmentation with residual nitrogen gas occurs when ions are accelerated from the C-trap into the HCD cell. The fragments are returned from the HCD cell as a single ion cloud into the C-trap. In CID collision, the ions are first collected as a package and thereafter moved by resonance back and forth in a collision gas until the ions break apart and produce fragments. The Orbitrap also contains a quadrupole that often serves as a broadband mass filter to reduce total ion abundance permitting longer injection times or to isolate the precursors for fragmentation. The quadrupole cannot be used in the scan mode because the Orbitrap and C-trap require ion clouds. Unlike QqQ instruments, the orbitrap detector does not monitor the incoming ions in a continuous manner. Instead it produces a data point after a sufficient number of ion oscillations in the mass analyzer has been monitored and processed (38).

1.7.3 AcquireX Methodology

AcquireX acquisition is an attractive strategy to acquire quantitative, complete MS data from the full scan data, as well as confirmation data from the MS/MS data (38). AcquireX requires an exclusion list, i.e. compounds present in a blank sample, and an inclusion list, i.e. compounds present in a representative sample. In AcquireX mode, the MS instrument performs a full scan, followed by MS/MS analysis on precursor ions selected from the inclusion list. When MS/MS data of the representative sample is available, it is aligned with the full scans of the samples by m/z and retention time. The selection of precursor ions for MS/MS analysis is dependent on the intensity of the ion. Thus, compounds with low abundance may not be selected for fragmentation and will have no MS/MS data associated with them.

2 Aims of the Thesis

The overall aim of this study is to develop a sample processing methodology for simultaneous extraction of lipids and metabolites from the same sample. The methodology will afterwards be used to explore the differences in the lipidome between people taking high dose vitamin D compared to placebo. In addition, the differences in the autumn compared to in the spring is also to be explored due to the lack of sunlight during winter in Northern Norway.

3 Materials and Methods

3.1 Materials

3.1.1 Chemicals

Table 3-1 List of chemicals

Chemical	CAS	Manufacturer
Methanol	67-56-1	Sigma-Aldrich
Methyl-tert-butyl-ether	1634-04-4	VWR International
Chloroform	67-66-3	Supelco
2-propanol	67-63-0	Supelco
Acetonitrile	75-05-8	VWR International
Ammonium formate	540-69-2	Supelco
Formic acid	64-18-6	Supelco

3.1.2 Materials and Equipment

Table 3-2 List of materials and equipment

Material/Equipment	Description	Manufacturer/Provider
Thermo Scientific™ Orbitrap IdX™ Tribrid™	MS-instrument	Thermo Fisher Scientific
Thermo Scientific™ Vanquish™	UPLC-system	Thermo Fisher Scientific
Acquity™ Premier BEH C18 1.7 µm, 2.1 x 100 mm	Column	Waters
MagNA Lyser Instrument	Cell lysis instrument	Roche
Biofuge fresco	Refrigerated centrifuge	Heraeus Instruments
Heidolph Reax top	Vortex	Heidolph Instruments
Stuart sample concentrator SBHCONC/1	Evaporator/concentrator with N_2	Cole-Parmer
Stuart block heater SBH200D/3	Evaporator/concentrator with heat	Cole-Parmer

CentriVap Concentrator	Evaporator/concentrator with centrifugal force, vacuum, and heat	Labconco
M-pact AX423	Scale	Sartorius Mechatronics
MagNA Lyser Green Beads	Vial and beads for cell lysis	Roche
Eppendorf tubes	Safe-Lock Tubes 1.5 ml	Eppendorf Research
HPLC vial	12x32 mm glass screw neck vial, cap, nonslit PTFE/silicone septa, Total Recovery	Waters
HPLC vial	12x32 mm glass screw neck vial, cap, nonslit PTFE/silicone septa	Waters
Micropipette	0.5-10 µl 10-100 µl 20-200 µl 100-1000 µl	Eppendorf Research
Pipette tip	10 µl 250 µl 1000 µl	Thermo Fisher Scientific
Laboratory bottles, round	Borosilicate 3.3 glass, with PP screw cap and pouring ring. 100 ml 250 ml 500 ml	VWR
Puranity PU 15 System	Ultrapure water system, purification of water	VWR

3.2 Study Design and Methods

3.2.1 Study Population and Recruitment

This study included healthy subject with serum 25(OH)D levels in the range 25-45 nmol/L. The participating subjects had either participated in previous vitamin D intervention studies performed by the research group or were recruited through advertisements in the local press and on billboards at UiT – the Arctic University of Norway and the University Hospital of North Norway (UNN) in Tromsø. Those who responded were contacted by phone by a study nurse and informed about the study. If they were still interested in participating after being informed about the study and there were no contradictions in their medical history, an appointment for the first visit was made. The consent form sent by mail as further information.

The study only included men between the age of 20 to 70 years and postmenopausal women over 60 years with BMI in the range 21-32 kg/m^2. Exclusion criteria were smoking, use of medication, use of vitamin D supplements or cod liver oil, vacation in a sunny country or use of solarium during the study period, development of any chronic disease and start of permanent or long lasting medication, dieting or new vigorous exercise/training, allergy to nuts or local anesthetics, disturbances of calcium metabolism (primary hyperparathyroidism), granulomatous diseases (Wegner's granulomatosis, sarcoidosis, tuberculosis), reduced kidney function (creatinine >115 µmol/L in males and 110 µmol/L in females), and renal stones in the last 15 years.

3.2.2 Intervention

The intervention was performed for two months during the time of the year with the lowest serum 25(OH)D levels. The inclusion period was from October until January and the last visits by the end of March. Subjects randomized to treatment group each received one box with 24 vitamin D_3 capsules (20 000 IU). Correspondingly, subjects of the placebo group each received a box with 24 identically looking placebo capsules. Directly after baseline procedures, the subjects were to take four capsules as a loading dose. Afterwards, two capsules were to be taken each week with the exception of the last day before the last visit. The subjects were contacted by phone after one month. The purpose was mainly to remind the subject to take the medication, but also to ask about adverse events. Unused study medicine was returned at the endpoint visit.

3.2.3 Randomization

Randomization to the vitamin D or placebo group was performed using a block randomization procedure and stratified according to gender and BMI (<27 kg/m^2 and >27 kg/m^2). Randomization was performed by the central randomization unit at the Clinical Research Center, University hospital of North Norway, which was informed of about gender, BMI and date for baseline visit after the screening by the study nurse.

The randomization numbers with treatment allocations were provided directly to the hospital pharmacy where the medication was prepared. The participants received the study medication at the end of the baseline visit. Only the pharmacy and the Clinical Research unit at the hospital had access to the randomization list. All investigators were kept blinded. All data were sent directly to the hospital's Clinical Research unit where they were merged and coupled to the randomization code. The final file without person identification was then sent to the principal investigators.

3.2.4 Samples

After blood samples for analysis of background characteristics were taken in fasting state, and 15 minutes rest, fat biopsies were taken from the SAT on the lower abdomen according to the procedure described by Mutch et al. (39), washed with phosphate buffered saline, immediately frozen in liquid nitrogen and stored at -80 ºC.

The participants were assigned an ID number which the samples were marked with either visit 2 (v2) or visit 3 (v3) for whether it was taken at baseline or endpoint, respectively. List of all samples can be found in the appendix.

3.2.5 Sample Preparation

The method used was taken from Matyash's (40) solvent extraction method with the use of Methyl-tert-butyl ether (MTBE) and Coman's (41) Simultaneous Metabolite Protein Lipid Extraction (SIMPLEX) method, with some slight modifications. As the method was going to be utilizing MagNA Lyser Green Beads to homogenize the sample, it was advantageous to be have the organic phase containing the lipids as the upper phase of the two-phase partitioning system like in Matyash's (40) extraction with the use of MTBE. This simplifies the sample handling. Metabolites were extracted from the remaining aqueous phase in the Green Beads tube. This was done with a SIMPLEX method, where both lipids and metabolites can be extracted from the same sample. As the aqueous phase was at the bottom of the tube, it made it

difficult to collect. It was for that reason decided to use chloroform which has a higher density. This way the aqueous phase will form the upper phase and end up above the beads, while the new organic phase consisting of chloroform will form the lower phase. Thus, the metabolites can be easily collected.

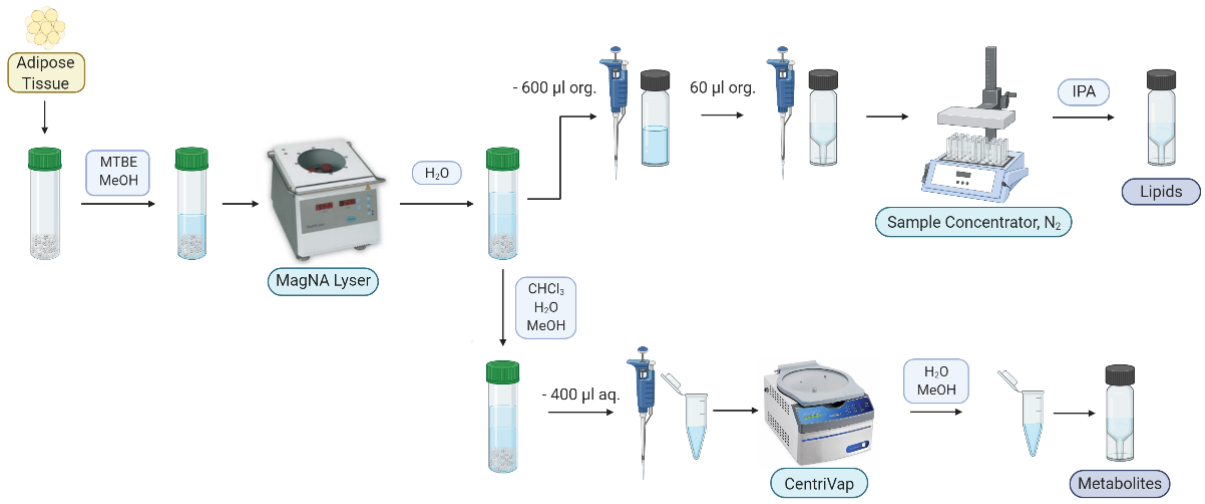

Figure 3-1 Workflow of sample preparation. Created with BioRender.com

3.2.5.1 Optimizing Method of Sample Preparation

The lipids were first tried extracted from fat biopsy by adding 700 µl of a mixture of MeOH and MTBE in 1:1 ratio and homogenized with MagNA Lyser Green Beads at 7 000 rpm for 30 seconds. 300 µl of Milli-Q water was then added to induce phase separation, though this did not work as planned. There was no visible phase separation at this point. Different ratios of the solutions were then tried to find the ratio that would give a visible phase separation that is also above the ceramic beads. From the results it was concluded that the ratio in which gave a visible phase separation was MTBE/MeOH/water in the ratio 7/3/2.5 v/v/v.

It was then decided to try three different methods, method A, B and C, to find out whether adding MTBE, MeOH and water in different steps is better that adding all simultaneously in one step. Method A added only MeOH before going through cell lysis in the MagNA Lyser, before adding MTBE and then water at last. Method B added both MeOH and MTBE before cell lysis, and then water for phase separation. Method C added all three in one step. After conducting this trial, it was decided to work with method B. Which showed a slightly elevated amount of extracted lipids compared to method C when compared in in Lipid Search. The sample from method A could not be analyzed as there was insoluble particles dispersed in the

solution that could not be removed with centrifugation. Thus, the sample could not be injected into the HPLC and was disregarded.

When running a full scan of the lipid samples in the orbitrap, the sample seemed to be very concentrated upon examination of the chromatogram. The sample was therefore diluted 1:10 and 1:100 for comparison. By examining both high intensity areas and low intensity areas, and comparing the undiluted sample, 1:10 and 1:100, it was determined that a 1:10 dilution seemed appropriate. During the period it was discovered contamination of polysiloxanes in the samples. From there on it was decided to have small bottles for the working solutions. The bottles were washed with MeOH and refilled with new solution every week, to lessen the risk of contaminations.

After extracting the lipids, the metabolites were to be extracted from the remaining aqueous phase in the Green Beads tube. By adding chloroform, the aqueous phase, that previously formed the lower phase, became the upper phase. This would ease the collection of the aqueous phase. After chloroform was added, it was found that the aqueous phase was very small, thus it was difficult to collect without possibly leaving a large amount of metabolites behind. It was then decided to add 200 µl of water. This made it possible to collect 400 µl from the aqueous phase. Though when the solvent was to be evaporated, water proved to be difficult to evaporate and very time-consuming. Consequently, half of the water was substituted with MeOH. This resulted in almost halving the evaporation time.

After evaporation the metabolites were reconstituted in 50 µl of a 20% MeOH solution, and analyzed on HPLC-MS, with a reverse phase column. But after attempting to identify the compounds through the software Compound Discoverer it was discovered that many of the compounds had up to 5 duplicates with different retention times, which was not ideal. Assuming this was caused by poor separation in the column, it was attempted to reduce the concentration of MeOH in the sample vial to 5%. The number of duplicates was reduced to 2 copies of the same compound for some compounds, and 3 for a very few, though there were no visible changes in the raw files.

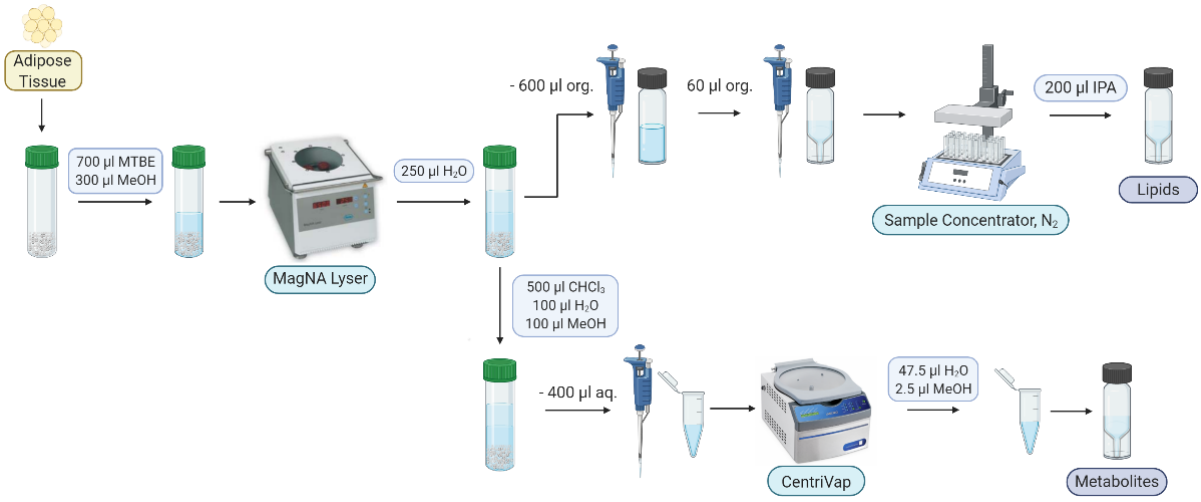

Figure 3-2 Workflow of final sample preparation with optimized volumes. Created with BioRender.com

3.2.5.2 Lipid extraction

The fat biopsy samples were prepared using solvent extraction with the use of MagNA Lyser Green Beads to homogenize the solid sample. 15 mg of sample was weighed out into the Green Beads tubes. In the tubes, 300 µl MeOH and 700 µl MTBE was added and then oscillated in the MagNA Lyser instrument at 7000 rpm for 30 seconds. 250 µl water was then added to induce phase separation. The tube was then shaken vigorously before centrifuged at 13 000 rpm (16 060 g) for 5 minutes. 600 µl of the upper layer of MTBE containing the lipids was then extracted from the tube into a vial. 60 µl, corresponding to 10%, of the organic phase was transferred to a total recovery vial where the solvent was evaporated (55ºC, N_2) and reconstituted in 200 µl isopropanol.

3.2.5.3 Metabolite extraction

Metabolites are extracted from the remaining aqueous phase in the Green Beads tube. 500 µl chloroform was added to form the new organic phase, which because of the density will become the lower phase in the two-phase partitioning system. 100 µl water and 100 µl MeOH was added to increase the volume of the aqueous phase. The tube was vortexed for 20 seconds, and then centrifuged at 13 000 rpm (16 060 g), for 5 minutes. 400 µl of the aqueous phase, which now forms the upper phase, was collected into an Eppendorf tube. The solvent was then evaporated (50ºC, centrifugal force, vacuum), reconstituted in 50 µl of a 5% MeOH solution and transferred to a total recovery vial.

3.2.5.4 Reproducibility

The reproducibility of the sample preparation was tested by preparing 6 samples with the method distributed over 3 days, in other words, 2 samples each day. For the lipids, it was only performed full scans for each sample. Masses of 20 different lipids were randomly picked out, where 10 were of high intensity and 10 were of low intensity. The intensity of each of the 20 lipids in the samples was compared and standard deviation was calculated. As for the metabolites a short AcquireX, DDA, with 3 deep scans was performed and data processed in Compound Discoverer.

3.2.6 HPLC-MS

The HPLC-MS analysis was performed with a Thermo Scientific™ Orbitrap IdX™ Tribrid™ Mass Spectrometer, connected to a Thermo Scientific™ Vanquish™ UHPLC.

3.2.6.1 Lipid analysis

The UHPLC utilized an Acquity™ Premier BEH C18 column (1.7 µm, 2.1 x 100mm), and a binary gradient (solvent A: 50% ACN, 1 mM NH_4FA, 0.01% FA, solvent B: 50/50 IPA/ACN, 1 mM NH_4FA, 0.01% FA) of 30 minutes, with a flow rate of 0.6 ml/min and at 60 ºC.

Table 3-3 UHPLC gradient for the analysis of the lipidome

Time (minutes)	**Flow (ml/min)**	**%A**	**% B**
-3.0	Equilibration		
-3.0	0.6	70	30
0.0	0.6	70	30
0.0	Run		
0.0	0.6	70	30
20.0	0.6	25	75
25.0	0.6	5	95
30.0	Stop Run		

MS-settings:

Table 3-4 Orbitrap IdX™ Tribrid™ settings for the analysis of the lipidome

MS Global settings	
Method Duration (min)	30
Expected LC peak width (s)	3
Data dependent mode	Cycle time
Cycle time (s)	1.5
MS OT	
Orbitrap resolution	120 000
Scan range (m/z)	250-1500
AGC target	400 000
Maximum injection time (ms)	50
Polarity	Positive
ddMS2 OT HCD	
Collision energy mode	Stepped
Collision energies (%)	25, 30, 35
Orbitrap resolution	15 000
Maximum injection time (ms)	50
AGC target	50 000
ddMS2 OT CID	
Collision energy mode	Fixed
Collision energy (%)	32
CID activation time (ms)	10
Orbitrap resolution	15 000
Maximum injection time (ms)	50
AGC target	50 000
ddMS3 OT CID	
Collision energy mode	Fixed
Collision energy (%)	35
Activation time (ms)	10
Activation Q	0.25
Orbitrap resolution	15 000
Maximum injection time (ms)	65
AGC target	50 000

3.2.6.2 Metabolite analysis

The UHPLC utilized an Acquity™ Premier BEH C18 column (1.7 µm, 2.1 x 100mm), and a binary gradient (solvent A: H_2O, 1 mM NH_4FA, 0.01% FA, solvent B: 50/50 IPA/ACN, 1 mM NH_4FA, 0.01% FA) of 16 minutes, with a flow rate of 0.5 ml/min and at 60 ºC.

Table 3-5 UHPLC gradient for the analysis of the metabolome

Time (minutes)	**Flow (ml/min)**	**%A**	**% B**
-2.0	Equilibration		
-2.0	0.5	99.5	0.5
0.0	0.5	99.5	0.5
0.0	Run		
0.0	0.5	99.5	0.5
1.0	0.5	99.5	0.5
15.0	0.5	5	95
16.0	0.5	5	95
16.0	Stop Run		

MS-settings:

Table 3-6 Orbitrap IdX™ Tribrid™ settings for the analysis of the metabolome

MS Global settings	**Positive**	**Negative**
Method Duration (min)	16	15
Expected LC peak width (s)	3	3
Data dependent mode	Cycle time	Cycle time
Cycle time (s)	0.6	0.6
MS OT		
Orbitrap resolution	60 000	60 000
Scan range (m/z)	70-800	70-800
AGC target	100 000	100 000
Maximum injection time (ms)	50	50
Polarity	Positive	Negative
ddMS2 OT HCD		
Collision energy mode	Stepped	Stepped
Collision energies (%)	20, 35, 50	20, 35, 50
Orbitrap resolution	30 000	30 000
Maximum injection time (ms)	54	54
AGC target	50 000	50 000

3.2.7 AcquireX

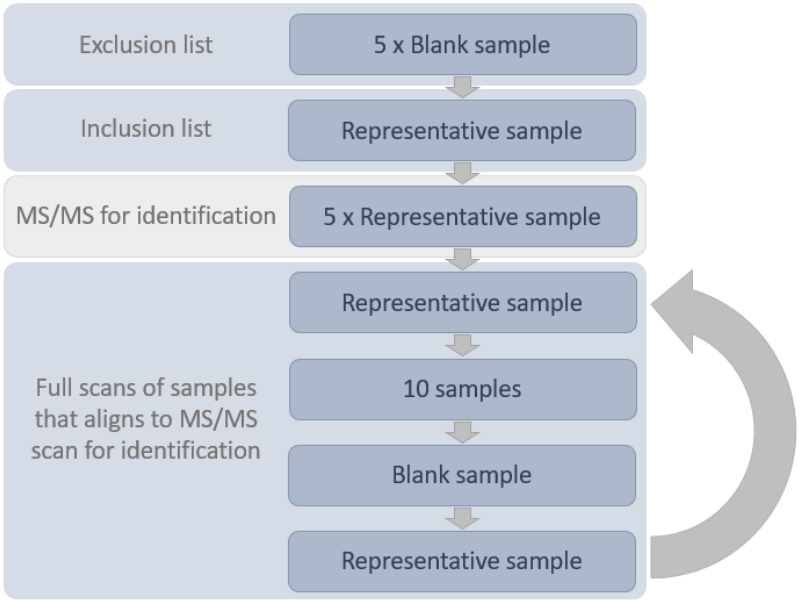

Figure 3-3 Schematic view of the AcquireX setup

The AcquireX run was started with 5 full scans of the blank sample where the last was used to create an exclusion list. Then a full scan of a representative sample (RS), consisting of 4 µl of 30 different samples, to create an inclusion list. Then followed by 5 deep scans of RS for identification with MS/MS. Thereafter, full scans of RS once, then 10 samples, followed by a blank and RS twice, before another 10 samples and repeating this cycle until all samples are injected. Before starting the AcquireX run, 2 blanks and 2 RS was run to equilibrate and as a control.

The time the samples were in the autosampler were minimized by changing out the samples twice a day, every 8-16 hours. Already injected samples were placed back into -80 ºC, and new samples were taken out and put into the autosampler. This was to reduce the risk of any alteration of the lipidome. RS and blank sample were in the autosampler for the duration of the entire run of approximately 80 hours.

The reproducibility of the AcquireX was tested by applying the masses of the same 20 lipids earlier used for the same purpose, into Skyline. Skyline registered the mass accuracy, retention time and peak area of each lipid in each of the RS, and generating simple graphs displaying the development and changes occurring during the analysis.

3.2.8 Data Analysis

The analysis of the data was performed using the software LipidSearch™ and Compound Discoverer™ for lipids and metabolites respectively for identification and quantification. Multivariate data analysis and other analyses was performed using SIMCA® software and MetaboAnalyst.

3.2.8.1 LipidSearch™

LipidSearch software processes LC-MS data to provide accurate lipid identification by aligning the peaks of the full scan of the samples and MS/MS data of the RS, and then integrates the peaks for relative quantification. The database contains defined structures and includes more than 1.5 million lipid ions and their predicted fragment ions (42).

Retention time tolerance was set to 0.2 minutes. LipidSearch has some problems integrating the peak area for compounds when the chromatographic peaks are not perfect, often integrating only a small corner or half of the peak. The integration for each lipid was looked over and manually integrated where it was necessary. Data was exported into an excel file.

3.2.8.2 SIMCA®

SIMCA Multivariate Data Analysis software is a data analytics tool used to gain information from large quantities of data. Multivariate data analysis analyzes multiple variables simultaneously and comprehend how various parameters interact with each other (43). Data generated in LipidSearch was imported into SIMCA which was used to perform principle component analysis (PCA), partial least squares discriminant analysis (PLS) and orthogonal partial least squares (OPLS). The analyses were first performed with the unprocessed dataset, with the peak area of the lipids as x-variable. PLS and OPLS was done with group affiliation (placebo baseline, placebo endpoint, vitamin D baseline and vitamin D endpoint), serum 25(OH)D level and SAT vitamin D level, as well as the ratios (endpoint/baseline) of the latter two as discriminant criteria. The peak areas were then calculated into ratios and a new PCA, PLS and OPLS was performed, with group affiliation, serum 25(OH)D ratio and SAT vitamin D ratio as discriminant criteria. In SIMCA, data was scaled with pareto scaling (mean-centered and divided by the square root of the standard deviation of each variable) and no normalizations steps were performed.

3.2.8.3 MetaboAnalyst

MetaboAnalyst is a comprehensive web-based platform dedicated for metabolomics data analysis. The objective is to enable high-throughput analysis for both targeted and untargeted metabolomics (44). MetaboAnalyst was used to perform statistical analyses, biomarker analysis, enrichment analysis as well as pathway analysis.

Statistical analysis module in MetaboAnalyst includes PCA, PLS and OPLS as well as other commonly used statistical methods. The discriminant criterion in PLS and OPLS in MetaboAnalyst is limited to being categorical. Therefore, only group affiliation was used as discriminant criterion in PLS and OPLS performed in MetaboAnalyst. Enrichment analysis and pathway analysis was performed to identify biologically meaningful patterns that are significantly enriched and to help identify the most relevant pathways involved in the conditions of this study. Biomarker analysis was performed for the 10 most influential lipids in the OPLS performed in SIMCA. This analysis provides the receiver operating characteristic (ROC) curve-based approach to identify potential biomarkers and evaluating their performance. In all analyses, the data was normalized by a pooled or average sample from the placebo group, filtered by interquartile range (IQR) and scaled with pareto scaling.

4 Results and Discussion

4.1 Sample Preparation

By extracting lipids and metabolites from the same sample, the amount of required sample is reduced, and sample handling errors reduced by fewer extraction steps. Thus, saving valuable sample material and enabling additional analyses, thereby gaining more information per sample. Though there are limitations for this method of extracting. Certain low abundance or very hydrophilic lipids will be hard to detect and may escape the hydrophobic phase. Similar behavior is likely for amphiphilic metabolites. This would be a disadvantage of the use of chloroform. Though chloroform would help remove any extra lipids that MTBE was not able to extract form the metabolite fraction, it could cause loss of unique compounds that would be removed from both lipid fraction and metabolite fraction. In such cases, an additional re-extraction would be beneficial.

The original Matyash (40) method of extraction operated was with the solvent ratios 10/3/2.5 v/v/v MTBE/MeOH/water. In this thesis the solvent ratio used was 7/3/2.5 v/v/v. It was first attempted with a ratio of 3.5/3.5/3 v/v/v, which would be similar to the solvent ratio of Bligh and Dyer's (45) extraction method of 2/2/1.8 v/v/v $CHCl_3$/MeOH/water. A study (46) comparing a similar solvent ratio to the original Matyash method and the conventional Bligh and Dyer across plasma, urine, and model organism D. magna. The study showed that their modified Matyash method had higher or comparable extraction yield and reproducibility than the original Matyash and Bligh and Dyer (46). When the similar solvent ratio of 3.5/3.5/3 v/v/v was attempted with adipose tissue samples in this thesis, the phase separation was not visible. For the sample of adipose tissue homogenization was needed, and the method applied in the thesis was with the use of MagNA Lyser Green Beads. As this method utilizes rigorous shaking with the ceramic beads, it may have leaded to the formation of an emulsion and thus no phase separation was found. Therefore, the solvent ratio used was 7/3/2.5 v/v/v. As there was a limited volume in the MagNA Lyser Green Beads tubes, as well as a minimum amount of water to cover all of the beads, the solvent ratio of the original Matyash method was not suitable with the use of MagNA Lyser Green Beads.

When testing different procedures for sample extraction, method A did not give the desirable results as it could not be analyzed because of the insoluble particles dispersed in the sample. A possible reason for this may be the small volume of liquid in the tube during the homogenizing, leading to the sample not being properly homogenized. The samples are homogenized by

rigorous oscillations, but without liquid it might be difficult to properly do so. The samples from both method B and C were homogenized and resulted in clear samples without particles. When comparing both in LipidSearch™ method B showed higher levels of extracted lipids than method C in all lipid classes except the glycerolipids where the levels were the same in both methods if not slightly higher in method C, figure 4-1. The difference between method B and C was whether water was added before or after homogenizing. It seems as though having water present during homogenization may cause less lipids to be extracted than when there is only organic solvents present, since lipids are poorly soluble in water.

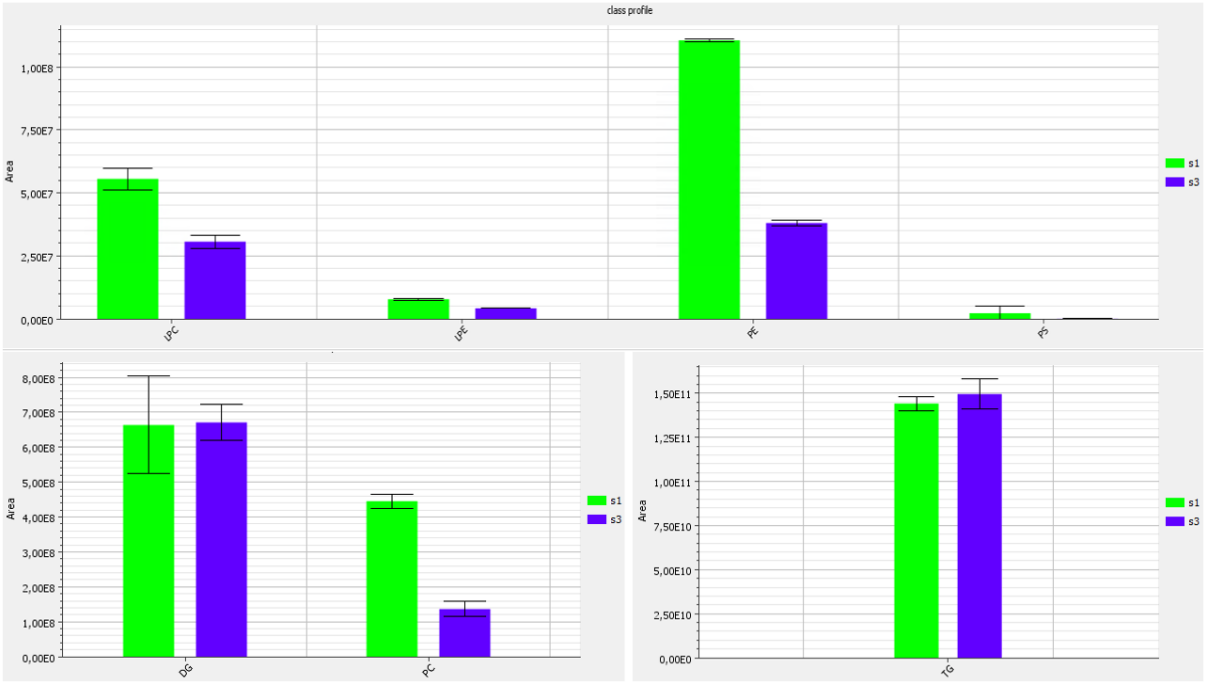

Figure 4-1 Class profile. Peak areas of the lipid classes LPC, LPE, PE, PS, DG, PC and TG, for method B and method C. Green=Method B, Blue=Method C.

Contamination of polysiloxanes found during the optimization of the sample preparation procedure was found in all samples, but in fluctuating intensities. After extended testing, it was later found that the intensity of the polysiloxanes signals increased with each repeating injection from the same vial. Subsequently, it was concluded that the polysiloxanes came from the caps of the vials. Each time the needle penetrates the septa it brings the polysiloxanes into the sample and accumulates for each injection, thus increasing the signal. The contamination was less with pre-slit caps, but for this experiment nonslit was necessary due to the possible evaporation of solvents from the vials. In addition, the contamination was of less importance when running an AcquireX method as the polysiloxanes would be excluded as it is present in the blank sample used for creating the exclusion list. Although, the polysiloxanes will fill the C-trap and thus

block for other more important ions that could have been analyzed. Additionally, this was only observed for the lipid samples and not in the metabolite samples. This seems to be explained by the solvents used for these samples. While the lipids are dissolved in the organic solvent IPA, the metabolites are dissolved in mostly water. IPA is able to dissolve the polysiloxanes the needle drags with it into the sample, while water is not able to. This way, polysiloxanes are able to accumulate in the lipid samples and not in the metabolite samples.

When testing the reproducibility of the method for sample preparation the intensity of the masses of 20 randomly picked lipids were noted for 6 samples prepared on 3 separate days, 2 samples each day. The result showed that the relative standard deviation (RSD) of the intensity of the lipids was 30% on average, though it varied from 8-78%. Lower intensity lipids showed a trend of higher RSD, while the high intensity lipids generally showed lower RSD. This was to be expected since when the intensity of the lipid is low, even small variations will result in high RSD. While for the high intensity lipids, big variation may not result in high RSD. Lipids extracted on day 1 seems to have a slightly higher intensity than that of day 2 and day 3.

Table 4-1 Intensity of 20 lipids from 6 samples, with calculated standard deviation. Red highlight shows sample with the highest intensity of the lipid, green highlight shows the lowest.

	Day 1		Day 2		Day 3				
	001	002	003	004	005	006	Average	Standard deviation	Relative standard deviation
TG 18:1 18:1 18:0	8.64E+08	8.30E+08	6.11E+08	6.51E+08	6.46E+08	6.62E+08	7.11E+08	107513100	15 %
TG 16:1 18:2 18:1	9.28E+08	9.01E+08	7.36E+08	7.59E+08	6.99E+08	7.49E+08	7.95E+08	94903459.72	12 %
TG 18:1 18:1 16:0	7.56E+08	8.07E+08	6.49E+08	6.93E+08	7.48E+08	6.93E+08	7.24E+08	56630969.15	8 %
TG 16:1 16:1 18:1	8.96E+08	8.49E+08	6.48E+08	6.55E+08	6.61E+08	6.76E+08	7.31E+08	111120505.2	15 %
TG 16:1 14:1 18:1	4.64E+08	4.47E+08	4.16E+08	3.10E+08	2.59E+08	2.62E+08	3.60E+08	93621934.75	26 %
TG 20:1 18:1 18:0	1.79E+08	1.91E+08	1.23E+08	1.41E+08	9.48E+07	8.24E+07	1.35E+08	43896605.79	32 %
TG 18:0 18:1 16:0	3.98E+08	4.16E+08	3.24E+08	3.35E+08	3.13E+08	2.98E+08	3.47E+08	48148381.77	14 %
PC 18:1 18:3	1.45E+06	1.08E+06	5.97E+05	6.77E+05	7.11E+05	8.88E+05	9.01E+05	320094.2049	36 %
DG 36:3e	1.85E+07	1.65E+07	1.16E+07	1.37E+07	1.24E+07	1.24E+07	1.42E+07	2730140.412	19 %
PC 16:0 18:2	3.73E+06	3.13E+06	1.84E+06	2.10E+06	2.20E+06	2.78E+06	2.63E+06	717272.6121	27 %
PC 16:0 18:1	6.90E+06	5.15E+06	3.28E+06	3.75E+06	3.92E+06	4.93E+06	4.66E+06	1312291.888	28 %
DG 36:4e	2.33E+07	2.37E+07	1.47E+07	1.74E+07	1.70E+07	1.67E+07	1.88E+07	3759787.228	20 %
LPC 16:0	1.21E+06	6.88E+05	1.08E+06	7.77E+05	1.62E+06	2.76E+06	1.36E+06	764181.7628	56 %
PC 16:0 16:1	1.45E+06	1.20E+06	6.48E+05	7.30E+05	9.06E+05	1.12E+06	1.01E+06	303991.4472	30 %
DG 1:16 4:20	1.60E+06	1.55E+06	9.72E+05	1.09E+06	7.54E+05	6.61E+05	1.10E+06	395297.2299	36 %
LPC 18:1	2.87E+05	1.76E+05	3.58E+05	2.66E+05	5.46E+05	7.77E+05	4.02E+05	221852.8041	55 %
LPE 16:0	9.46E+04	5.87E+04	6.54E+04	5.91E+04	1.44E+05	3.02E+05	1.21E+05	94647.14822	78 %
DG 18:2 18:2	4.65E+04	5.67E+04	4.13E+04	4.71E+04	3.50E+04	3.70E+04	4.39E+04	7929.859183	18 %
DG 18:0 22:5	1.76E+04	1.86E+04	1.21E+04	1.70E+04	1.16E+04	1.41E+04	1.52E+04	2977.694858	20 %
LPE 18:2	8.09E+03	6.61E+03	1.46E+04	1.97E+04	1.62E+04	3.26E+04	1.63E+04	9396.277987	58 %
									Average
Sum	4.54E+09	4.49E+09	3.54E+09	3.58E+09	3.46E+09	3.47E+09			30 %

Correspondingly, 6 metabolite samples were prepared, 2 samples each day for 3 days. Reproducibility of the extraction of metabolites were tested by performing a short AcquireX and data processed in Compound Discoverer 3.1. The data showed good reproducibility of the sample preparation method. None of the 285 identified metabolites had a significant change

between the days when the p-value had been adjusted using Benjamin-Hochberg correction for the false discovery rate. Results showed that the RSD of the area of the metabolites was on average 32%, though it varied from 2-108%. Only 4 out of 285 metabolites had an RSD over 100%. The metabolites also indicate a trend of higher RSD in lower intensity metabolites, and lower RSD in higher intensity metabolites, like seen in lipids.

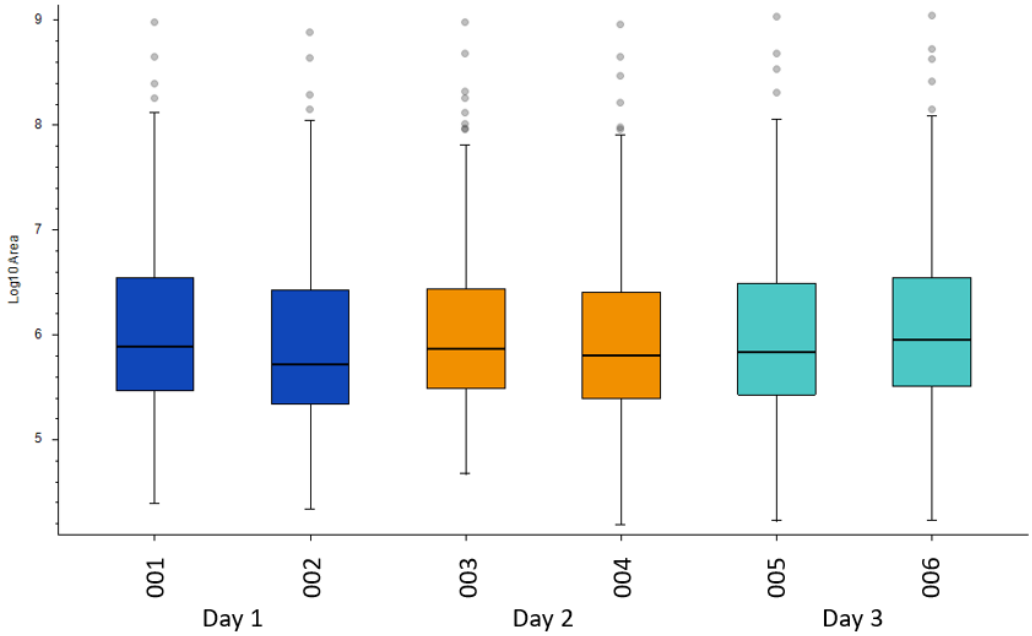

Figure 4-2 Box plot of area under the peak for all metabolites in 6 samples.

Metabolite identification was not optimized in the current project and it was decided to not include the metabolites in the current project due to time limitations and dependency of other larger projects to establish standardized LC conditions for both reverse phase and HILIC chromatography. Prepared metabolite fractions are stored at -80ºC awaiting instrument method development and validation prior to analysis.

4.2 AcquireX

When testing the reproducibility of the AcquireX run, the results showed that mass accuracy was mostly at an adequate level, although one of the lipids had a mass error almost reaching 3 ppm. However, a large shift in retention time where the trend showed a decrease in retention time from the first sample to the last was observed, figure 4-3. At the best the decrease in retention time from start to end was 0.5 minutes, but at worst the difference was at 3.4 minutes. At the same time, the pressure also decreased with the same trend as the retention time, where the pressure had decreased from 667 bar in the first RS full scan to 608 bar in the last. Therefore, it was suspected that it was either a problem with the pump or there was a leakage. Through further investigation it was found that there was a leakage of mobile phase A. This led to an increase in percentage of mobile phase B which caused the decrease of retention time. Thus, causing the compound to elute earlier each run.

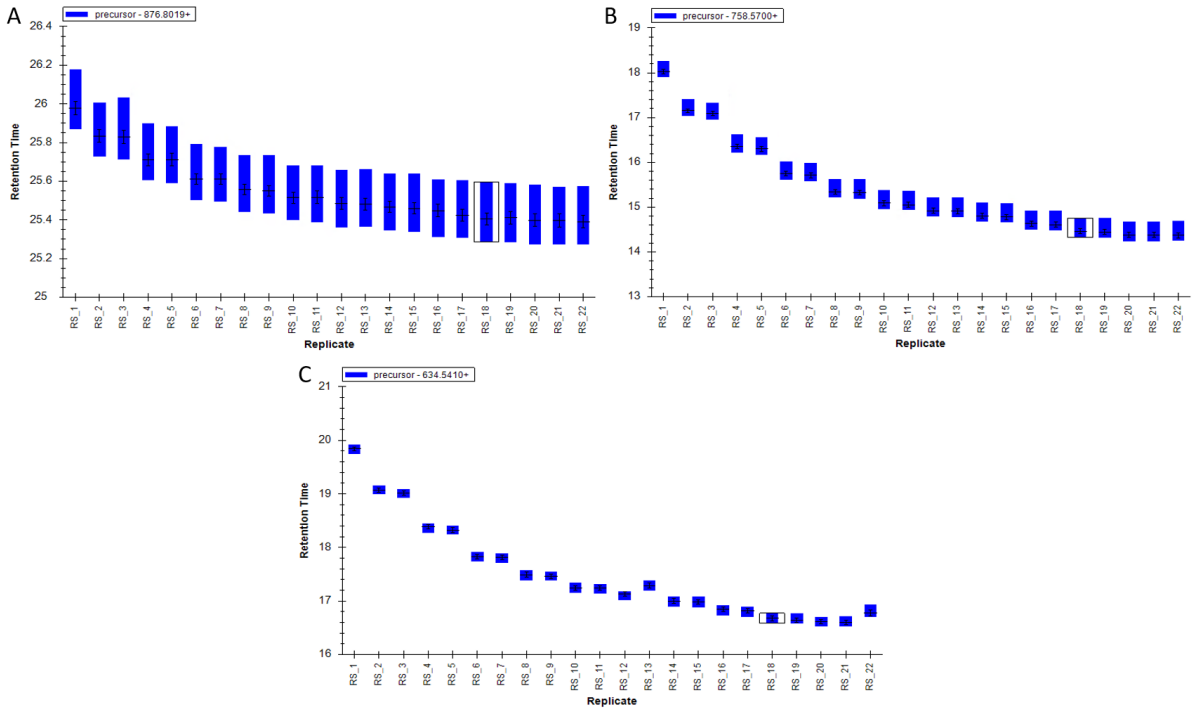

Figure 4-3 Retention time profile of the first AcquireX run. A: TG 18:1 18:1 16:0, B: PC 16:0 18:2, C: DG 18:2 18:2. Generated with Skyline.

This caused a problem when analyzing the data with LipidSearch™. Since the retention time differed greatly, LipidSearch™ was not able to align the sample data with the MS/MS data and therefore not able to identify and quantify the compounds. For this reason, it was necessary to redo the AcquireX run after the leakage was repaired. At the second attempt, the stability had improved, figure 4-4. The retention time did not deviate more than 0.1 minutes.

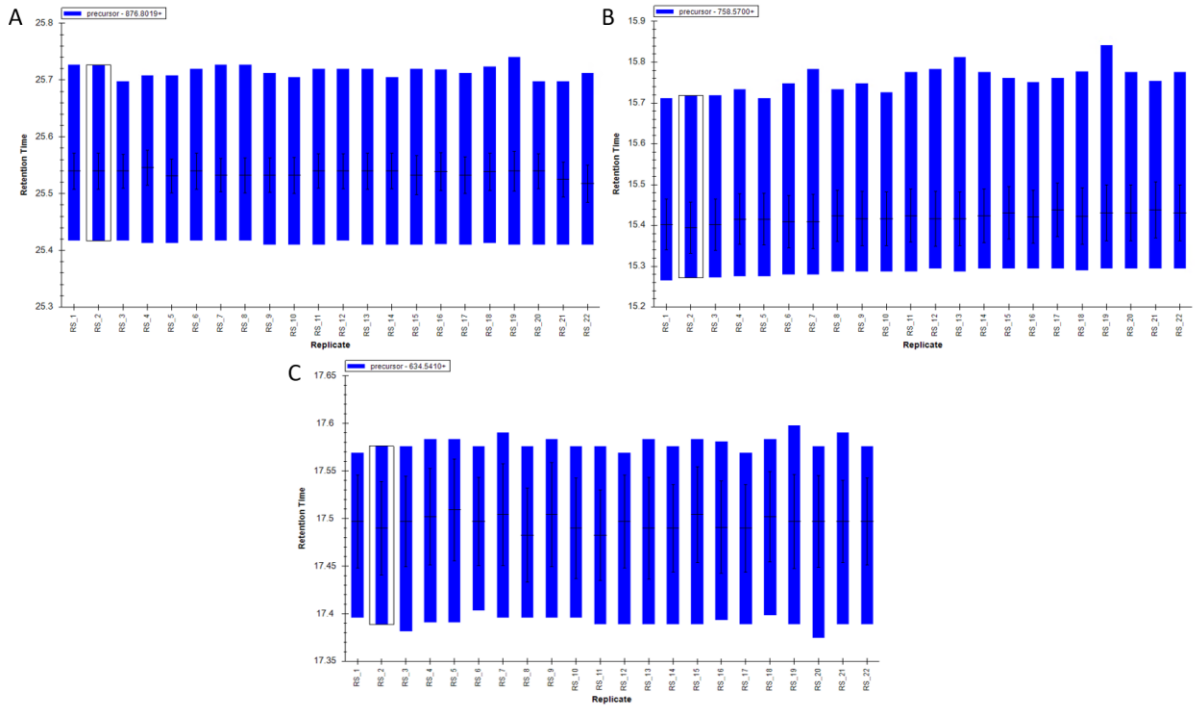

Figure 4-4 Retention time profile of the second AcquireX run. A: TG 18:1 18:1 16:0, B: PC 16:0 18:2, C: DG 18:2 18:2. Generated with Skyline.

The peak area was adequately reproduced throughout the run with the exception of the last five RS that had an increase in peak area. The suspected cause for the increase is that the vial with the RS had been vortexed once as it was observed precipitation at the bottom of the vial. The time of the vortexing matches that of the observed change in peak area. The increase was most prominent in PCs and less prominent in the TGs, which can possibly be attributed to the abundancy of the TGs compared to the other lipid classes or simply the different properties of the lipids.

Though it is unknown whether it was lipids that precipitated, it would be reasonable that mixing the RS cause possibly precipitated lipids to dissolve back into the sample and thereby increasing concentration and peak area. Precipitation was not observed for the samples, nor the blank sample. The RS is the only sample containing lipids that is in the autosampler at 5ºC for the entire run of more than 80 hours and is injected repeatedly at a total of 28 times. Whereas the other samples stay in the autosampler for maximum 16 hours and injected only once. It was done a short test for the temperature in the autosampler on beforehand, where it was tested

whether the samples could be in 5ºC as this was preferred over 20ºC for the convenience for the many users of the orbitrap. An equivalent lipid sample was placed in 5ºC for 30 minutes and no precipitation was observed. Compared to the 80 hours the RS was kept in the autosampler, 30 minutes is a short time. Therefore, this test may not be representative for the experiment. For this reason, it may have been more advantageous to aliquot the RS and changed out together with the samples.

The peak area did not show any substantial decrease even supposing that the lipids precipitated midway, and it is therefore uncertain whether the precipitation consisted of lipids. The evaporation of IPA was tested before, where 1% of IPA evaporated in 24 hours. This was tested with a vial of IPA left in the autosampler for 24 hours, the vial was capped with a nonslit cap that had been penetrated once. It may have been possible that the evaporation and precipitation happened at the same pace and thus keeping a constant concentration. Alternatively, the lipids could have been sticking to the side of the vial as IPA evaporated, keeping a constant concentration in the sample. In this case, vortexing would dissolve the lipids on the side of the vial into the sample again and thereby increasing the concentration. The increase would then be more prominent in lipids with higher affinity to the glass as there will be more of these against the glass wall of the vial.

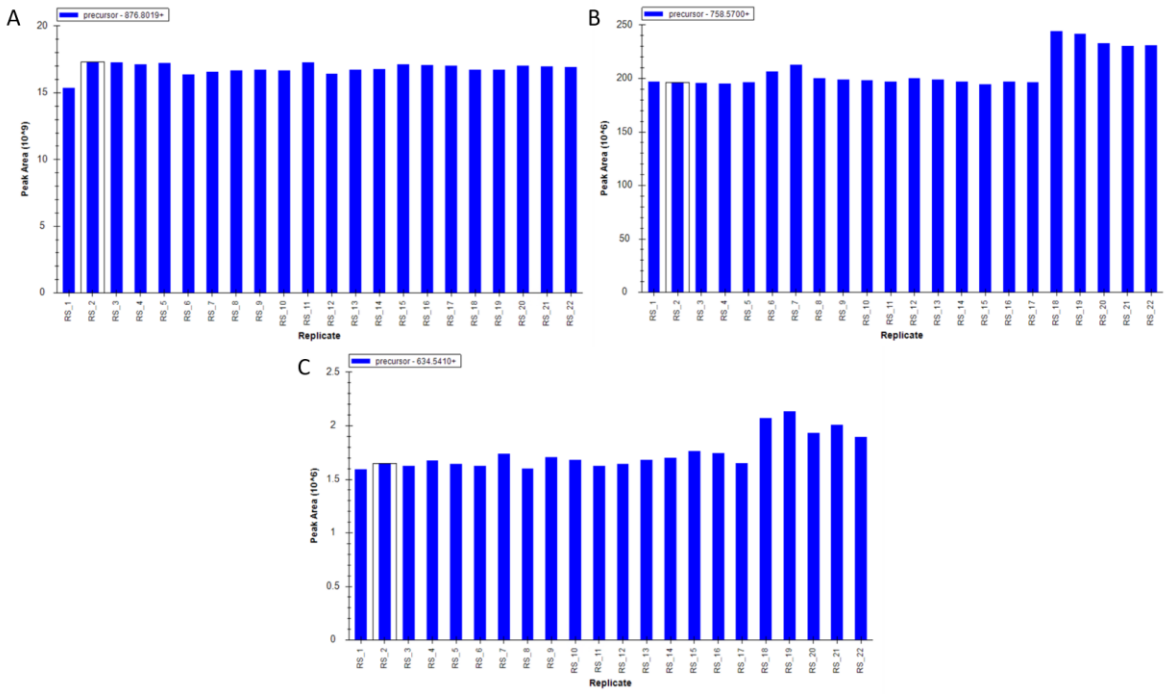

Figure 4-5 Peak areas of the second AcquireX run. A: TG 18:1 18:1 16:0, B: PC 16:0 18:2, C: DG 18:2 18:2. Generated with Skyline.

The majority had a mass error that stayed below 2 ppm, with a few exceptions where the highest mass error did not surpass 3 ppm.

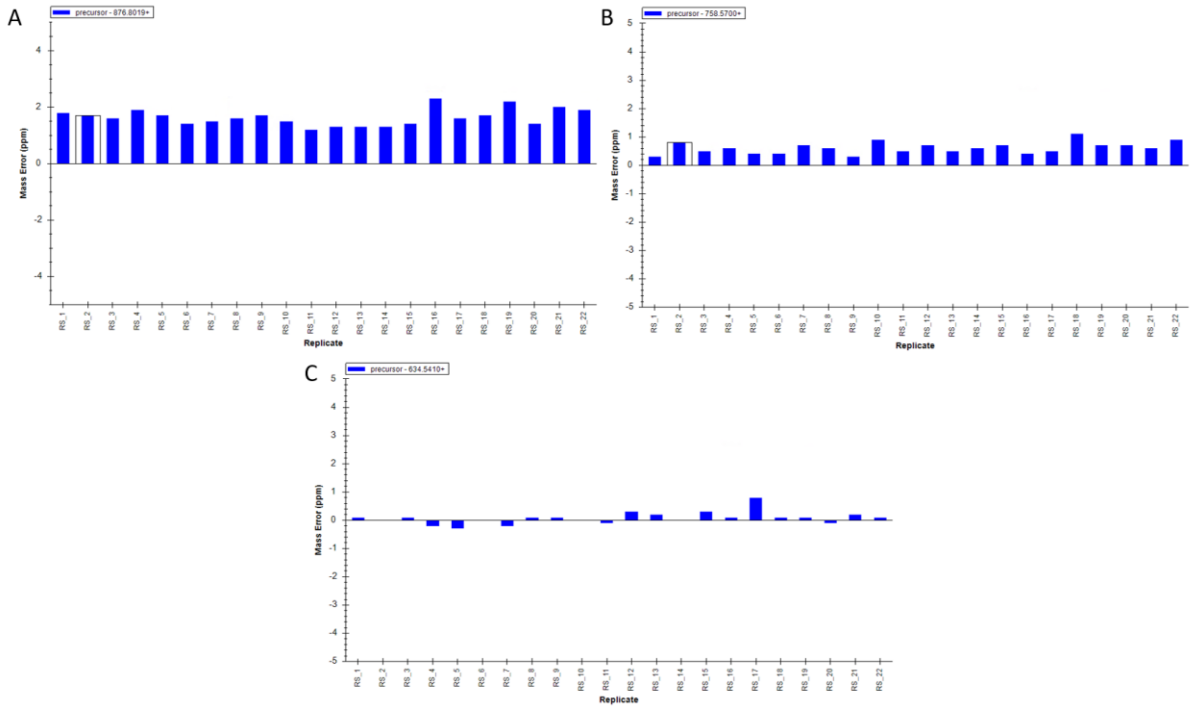

Figure 4-6 Mass errors of the second AcquireX run. A: TG 18:1 18:1 16:0, B: PC 16:0 18:2, C: DG 18:2 18:2. Generated with Skyline.

4.3 Identification and Quantification

As LipidSearch does not optimally integrate peaks that are not chromatographically perfect, it causes for the quantification to be inaccurate. When integrating the peak area for the same compound, one of the samples may only have half of the peak integrated while another has the whole peak integrated, figure 4-7. As a result, some samples may be perceived as having much lower intensity of a compound than they actually do and cannot represent the reality. Therefore, the data could not be used as it was and needed to be processed. The reintegration was done to the best ability with the time available. Ideally, each sample should be integrated separately for the best accuracy, but due to time constriction this was not possible. Therefore, all samples were reintegrated as a bulk for each compound, with a few exceptions. Since the retention time did not vary, this was unproblematic most of the time.

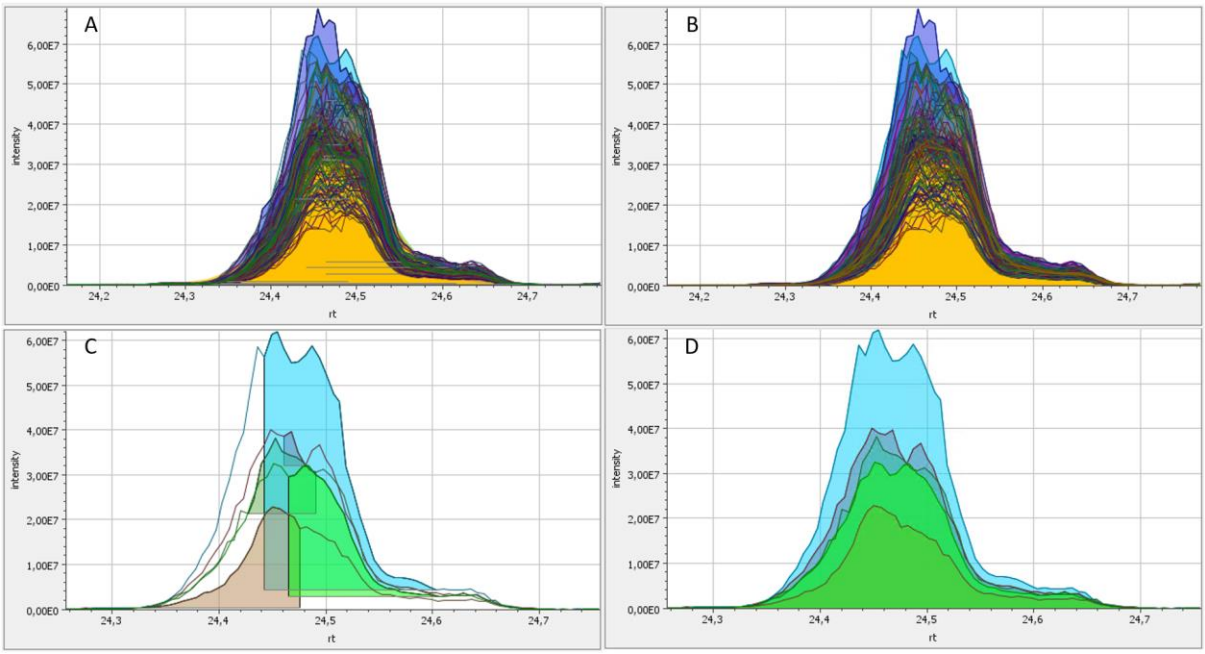

Figure 4-7 Integration of TG 14:0 18:2 15:0 in LipidSearch. A: All samples integrated by LipidSearch. B: All samples manually integrated. C: 5 of the samples integrated by LipidSearch. D: 5 of the samples manually integrated.

The retention time tolerance for the alignment in LipidSearch was set to be 0.2 minutes. The deviation of the retention time was less than 0.1 minutes for the 20 tested lipids. In the case of these 20 lipids, the retention time tolerance could be set to 0.1 minutes, but because the retention time deviation of all the remaining lipids is unknown 0.1 minutes was added. Looking through the dataset there were observed duplicates for some of the lipids, some of which being isomers and some not. As an attempt to remove duplicates an alignment with the retention time tolerance adjusted to 0.3 minutes was run to compare. When comparing the two alignments, there were less duplicates with 0.3 minutes retention time tolerance but also losing unique lipids.

Consequently, it was chosen to proceed with the alignment with 0.2 minutes retention time tolerance. With 0.2 minutes retention time 633 lipids were identified, where 511 of these were triglycerides (TG), 73 phosphatidylcholines (PC), 22 phosphatidylethanolamines (PE), 18 diglycerides (DG), 6 phosphatidylserine (PS), 2 lysophoshatidylethanolamines (LPE) and 1 lysophosphatidylcholine (LPC).

The identification of some of the lipids were not complete. LipidSearch would be able to define which lipid class as well as the total number of carbons in the fatty acid chains and number of double bonds, but not how these are distributed. For example, it would identify a lipid as PC 32:2 but not be able to tell how the 32 carbons and double bonds are distributed over the two fatty acid chains on a PC. This lipid could for example be PC 16:1 16:1 or PC 14:0 18:2. This was seen in all of the lipid classes, but it was most prominent among the phosphoglycerides where the majority did not have the fatty acid chains identified. The reason for this is that in the MS/MS these lipids almost exclusively lose their phosphate head group. Taking PCs as an example, these showed an intense fragment at m/z 184 which is attributed to the choline phosphate headgroup. It might have been possible to acquire a better identification of these in LipidSearch by adjusting the intensity threshold. By lowering the intensity threshold, it could be possible to find the less intense fragments of the fatty acid chains. However, this would also imply an increase of false positive identifications of other lipids.

4.4 Multivariate Data Analysis

The omics provide a comprehensive, or global, assessment of a set of molecules and the goal is to determine the relative differences between two or more systems or conditions. However, with such global analyses with high information content, it is a challenge to efficiently form biologically relevant conclusions from the datasets. An approach to data interpretation in omics is therefore the use of multivariate data analysis (MVA), such as principal component analysis (PCA) and partial least squares regression analysis (PLS).

The main objective of PCA and PLS is to identify differences between classes from a multivariate dataset. The aim of PCA is to achieve a linear transformation with lower dimensionality output data that neglects as little of the variance in the original data as possible. While the unsupervised nature of the PCA algorithm enables unbiased dimensionality reduction, it only reveals group clusters when within-group variation is sufficiently less than between-group variation. Therefore, supervised forms of discriminant analysis such as PLS (or PLS-DA) which rely on the class membership of each observation are also commonly applied in omics experiments. The utilization of class memberships allows the algorithm to expose the separation between classes better. However, variations that are not directly correlated with the class information is still present in the scores. This can complicate the interpretation of PLS scores and loading plots. Orthogonal partial least squares (OPLS) separates predictive from uncorrelated variation by incorporating an orthogonal signal correction into the PLS model, making interpretation easier (47).

In this study, the differences in the lipidome between the experimental groups are yet unknown. For exploratory studies like this, the initial application of PCA provides an informatory first look at the dataset structure and also the relationships between the groups. Ideally, the results of PCA analyses would be utilized to formulate an initial biological conclusion, which PLS or OPLS then can verify and test in more detail (47).

MVA was first performed with peak area as x-variables. The results from this showed no separation between placebo group and vitamin D group, before and after intervention. Ideally the vitamin D group at endpoint should have separated from placebo baseline, endpoint, and vitamin D baseline. However, neither the PCA, PLS nor the OPLS showed separation between the groups, regardless of discrimination criterion. This could possibly be because of large individual differences in lipid abundancy among the participants. Therefore, the change from baseline to endpoint was calculated by dividing the peak area at endpoint, by the peak area at

baseline to get a ratio. MVA was performed again with the ratios as x-variables. While the PCA displayed no separation of the samples, the groups could be distinguished from each other when OPLS was applied, figure 4-8.

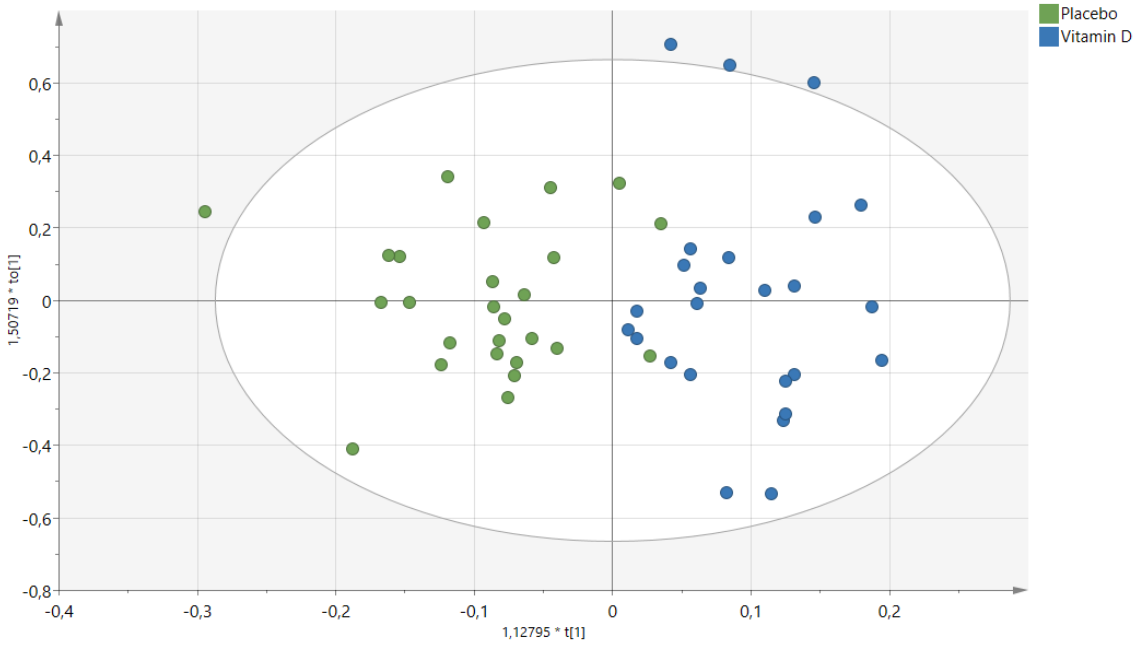

Figure 4-8 OPLS with peak area ratio (endpoint/baseline) as x-variable and group affiliation as discrimination criterion. Colored by group affiliation.

This result shows that vitamin D has an effect on the lipidome in human AT. In spite of this, evaluating the predictive validity of the OPLS model using the Q^2 values showed no predictability. Q^2 indicates how well the model predicts new data. A large Q^2 indicates good predictivity. Generally, a model with $Q^2>0.5$ is regarded as a predictive model. On the other hand, a $Q^2<0$ represents a lack of predictive relevance. Q^2 value for this model was -0.931, signifying no predictivity. The reason for low Q^2 value could be due to noise in the data, poor relationship between x- and y-variable or dominating outliers (48).

The same analysis was done with both change in serum 25(OH)D and SAT vitamin D in the form of ratios as discrimination criterion. It was still not possible to discriminate the groups from each other in the unsupervised PCA and was only clear in the supervised OPLS. Though the separation of the groups was much more visible with serum 25(OH)D, than SAT vitamin D as discrimination criterion, figure 4-9. The model with serum 25(OH)D as discrimination criterion showed similarity to the model with group affiliation as discrimination criterion. Whilst using SAT vitamin D showed less separation. Both these models also showed no

predictability with a Q^2 value of -1.16 and -0.697, for serum 25(OH)D ratio and SAT vitamin D ratio respectively.

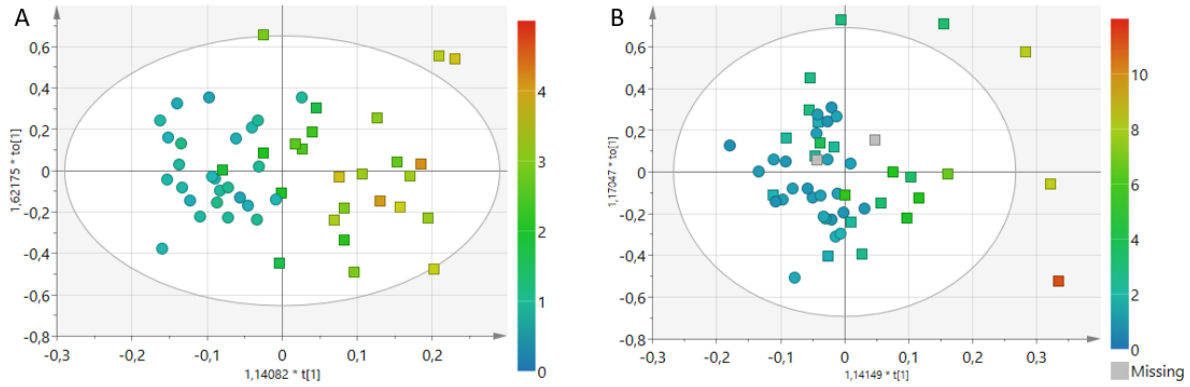

Figure 4-9 Supervised MVA of factors between lipid concentrations at baseline and at endpoint. A: OPLS with serum 25(OH)D ratio as discrimination criterion. Colored according to serum 25(OH)D ratio. B: OPLS with SAT vitamin D ratio as discrimination criterion. Colored according to SAT vitamin D ratio. □=Vitamin D, ○=Placebo.

This would indicate that the relationship between lipidome and vitamin D level in AT is poorer than between the lipidome and 25(OH)D in serum, meaning that the lipids in AT may be affected not by vitamin D in AT but somewhere else. There is a possibility that vitamin D or 25(OH)D has a mechanism of action that affects the lipids in the AT in the liver, a primary site of lipogenesis. 25(OH)D is the most abundant endogenous vitamin D metabolite and is produced in the liver. A study suggests that, even though 25(OH)D is generally considered biologically inactive, it acts together with $1,25(OH)_2D$ to control lipogenesis, as the study identified 25(OH)D as an inhibitor of sterol regulatory element-binding protein (SREBP) activation, a master regulator of lipogenesis. SREBPs are transcription factors that control the lipid homeostasis and is majorly expressed in the liver. The activation of SREBP is regulated by a negative feedback loop in which sterols bind to SREBP cleavage activating protein (SCAP). The stability of SREBPs depends on SCAP, the escort proteins. SCAP is necessary for activation of SREBP. It was found that 25(OH)D mediated degradation of the SREBP-SCAP complex is non-genomic and is independent from VDR. In addition, non-hydroxylated vitamin D had no effects on SCAP levels, indicating that hydroxylation is required (49).

While investigating the dataset it was seen that there were some inconsistencies in the SAT vitamin D compared to what was initially expected. Comparing the SAT vitamin D levels to serum 25(OH)D levels, the average serum 25(OH)D level at baseline was 35.8 nmol/l and 35.3 nmol/l in placebo and vitamin D group, respectively. At endpoint the serum 25(OH)D level reduced to 27.4 nmol/l in placebo group and increased to 99.8 nmol/l in the vitamin D group.

The placebo group had a slight decrease in serum 25(OH)D, whilst the vitamin D group had an increase with the ratio ranging from 1.68 to 4.14 and an average at 2.9.

On the other hand, average SAT vitamin D level at baseline was at 20.8 ng/g and 25.1 ng/g in placebo and vitamin D group respectively. At endpoint the average SAT vitamin D level remained at 20.7 ng/g in the placebo group and increased to 71.9 ng/g in the vitamin D group. But the level of vitamin D in AT varied greatly and a few of the individuals had a higher level of vitamin D at baseline than many of the individuals in the intervention group at endpoint. In the placebo group, the change in SAT vitamin D level was minimal, and most participants had a decrease in SAT vitamin D level. Though there is a visible increase in level of vitamin D in the intervention group from baseline to endpoint, the increase varies critically. The ratio of vitamin D in SAT from baseline to endpoint varied from 1.3 to 11.9 times. That would mean that some of the participants only had a barely increased SAT vitamin D level even after taking high doses of vitamin D for 2 months, meanwhile others had almost a 10-fold increase and one individual that had more than that, figure 4-10.

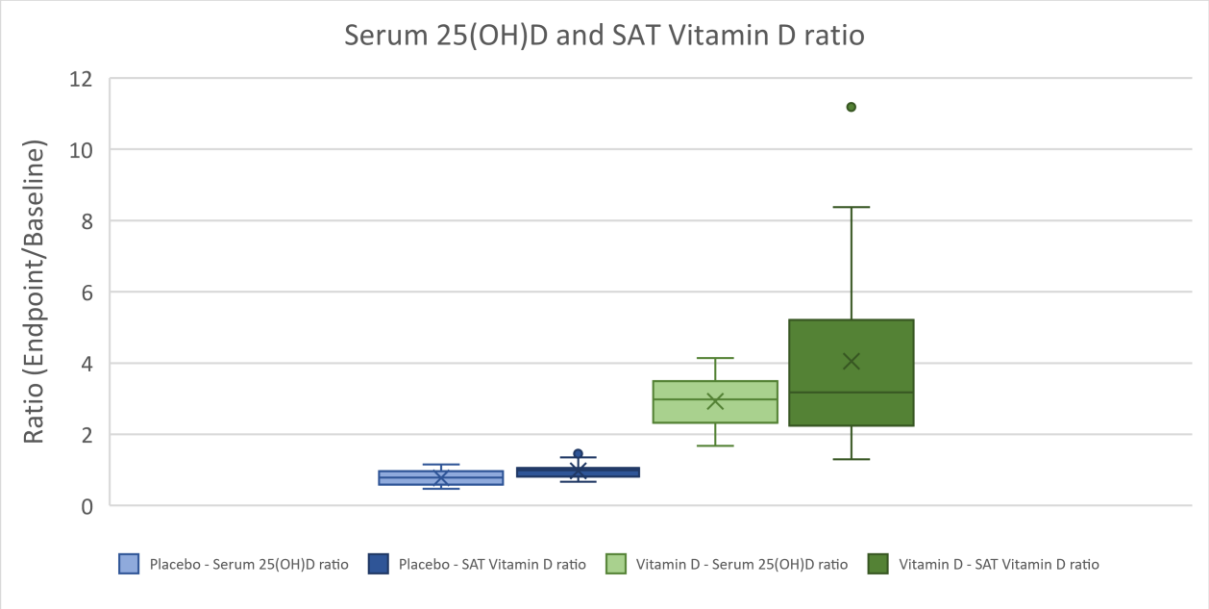

Figure 4-10 Box plot of the change in serum 25(OH)D and SAT vitamin D from baseline to endpoint as a ratio (endpoint/baseline) in placebo and vitamin D group.

Vitamin D is lipophilic and therefore accumulates in AT. This was demonstrated with the use of radioactive isotopes by Rosenstreich et al. (22). It was found that subjects supplemented with 20 000 IU per week for 3-5 years increased vitamin D levels in SAT by approximately 6-fold compared with placebo. Though, the amount of vitamin D present in SAT varied substantially, ranging from 3.6 to 118 ng/g in placebo group and from 89 to 510 ng/g in the vitamin D group.

This suggest a large individual variability due to several possible factors, such as differences in intake, compliance and skin production (23). A study showed that there was a relation between serum 25(OH)D level and SAT vitamin D level at baseline, but not after 3 months of supplementation of 2000 or 4000 IU/day. It was therefore suggested that adipose tissue is supplying vitamin D to the plasma for conversion to 25(OH)D when there is little to no recent vitamin D input (50). When serum 25(OH)D levels decrease after discontinuation of vitamin D supplement, AT vitamin D stores acquired during supplementation may be slowly released form AT (51). As it has been found that obese individuals have lower circulating 25(OH)D levels as well as attenuated UV exposure induced increase in 25(OH)D than individuals without obesity, it has been suggested that vitamin D is less bioavailable in obese individuals. Thus, it appears as though vitamin D can be trapped in AT (52). The participants in this thesis has a BMI between 21-32 kg/m^2. A BMI of 30 kg/m^2 or above is considered obese, though BMI is just an indication as it does not take fat and muscle percentage into consideration. It would be possible that the variability of vitamin D levels in AT and the poor correlation between serum 25(OH)D and SAT vitamin D could be because of the differences in BMI. It is possible that the trapped vitamin D is mobilized by physical activity along with stored lipids, as physical activity is a strong stimulus for lipid mobilization from AT. Studies indicate that exercise has a direct and causal effect on 25(OH)D concentrations possibly through mobilization with lipolysis as a possible key mechanism (52). Therefore, another possible factor could be the individuals' level of exercise. This is could not be further investigated as the individual BMI of each of the participants and level of physical activity was not available for this thesis. Though, fat percentage in the individuals may be a more interesting factor worth investigating.

To investigate which of the lipids that was responsible for the separation between the groups, a variable importance for the projection (VIP) plot was generated in SIMCA. The VIP plot summarizes the importance of the variables both to explain X and to correlate to Y.

Table 4-2 List of 20 most influential lipids for OPLS model with group affiliation as discrimination criterion.

#	Lipid	Average ratio Placebo	Average ratio Vitamin D	p-value	
1	TG 18:0 16:0 18:0	2.88	11.77	0.40	Increase
2	TG 48:0	2.70	4.67	0.44	Increase
3	PC 37:5e	1.24	1.89	0.45	Increase
4	TG 18:0 18:1 18:2	0.98	1.60	0.08	Increase
5	TG 4:0 18:1 16:0	0.89	1.42	0.16	Increase
6	TG 4:0 18:1 14:0	0.93	1.43	0.16	Increase
7	TG 16:1 18:1 18:1	0.99	1.30	0.11	Increase
8	TG 10:0 10:0 12:1	1.15	1.62	0.40	Increase
9	TG 4:0 16:0 18:2	0.90	1.36	0.19	Increase
10	TG 4:0 16:0 20:4	0.87	1.35	0.14	Increase
11	TG 18:1 18:3 22:1	0.94	1.14	0.05	Increase
12	TG 4:0 14:0 16:0	1.14	1.00	0.44	Decrease
13	PS 18:0 20:4	1.07	1.34	0.21	Increase
14	TG 16:0 14:0 20:3	1.07	1.35	0.25	Increase
15	TG 18:0 14:0 18:3	1.11	0.96	0.16	Decrease
16	PE 40:8e	0.96	1.14	0.01	Increase
17	TG 19:0 18:1 18:2	1.12	0.97	0.37	Decrease
18	TG 4:0 16:0 20:5	0.87	1.26	0.15	Increase
19	PC 20:4e 18:0	0.93	1.10	0.10	Increase
20	TG 18:3 18:3 18:3	0.96	1.13	0.18	Increase

*e - ether lipid

Three out of these lipids are incompletely identified, TG 48:0, PC 37:5e and PE 40:8e. TG 48:0 and PC 37:5e are the second and third most important lipids for the separation in the model, but as they have not been completely identified there is unfortunately not possible to know what lipid this is. Out of the 20 lipids, 17 showed an increase in ratio in the vitamin D group compared to placebo, while 3 showed a decrease. Nevertheless, only two of the lipids showed significant difference between vitamin D group and placebo group ($p \leq 0.05$), PE 40:8e and TG 18:1 18:3 22:1. Regrettably, PE 40:8e was not completely identified and the distribution over the fatty acids are unknown.

An interesting observation of these results was that 6 of the lipids contained butyrate, a four-carbon short-chain fatty acid (SCFA), and 5 of these were upregulated in the vitamin D group, though not significant. SCFAs, such as butyrate, are organic acids produced in the intestinal lumen by bacterial fermentation of partially or nondigestible polysaccharides. Butyrate has received attention for its beneficial effects on intestinal homeostasis and cellular energy metabolism. Butyrate has also been shown to play an important role in modulating immune and inflammatory responses and intestinal barrier function. Butyrate has shown to exert its anti-

inflammatory effects through inhibition of NF-κB, a transcription factor that regulates the expression of a variety of genes involved in inflammation and immunity, and upregulation of PPAR-γ, a member of the nuclear hormone family whose activation is thought to exert anti-inflammatory effects (53).

In genetically predisposed patients with inflammatory bowel disease there is an abnormal immune response to gut microbiota. This presents itself with less diverse and imbalanced gut microbiota composition, with a lower abundancy of butyrate producing species. It has been shown that vitamin D supplementation and the anti-inflammatory effect of VDR are directly associated with the gut microbiota (54). Schäffler et al. (55) reported that vitamin D supplementation temporarily increased the abundance of beneficial bacteria in remission Crohn's disease patients, but not in healthy controls. Among these is *Faecalibacterium*, whose characteristic is producing butyrate which has been shown to be a way to reduce inflammation. This study only had 17 participants, 7 with Crohn's disease and 10 healthy controls with vitamin D deficiency. All the participants in both groups received a total of 300 000 IU of vitamin D supplementation over the course of 4 weeks (55). The results of this thesis indicate that the participants in the vitamin D group show elevated levels of butyrate in the form of TG in SAT, compared to the placebo group. The mechanism for this could perhaps be attributed to the increase of beneficial bacteria in the gut microbiota.

The participants of this thesis are healthy subjects with no chronic diseases. Schäffler et al. showed no increase in the abundance of beneficial bacteria in healthy subjects, and in participants with Crohn's disease showed an increase that would decrease again towards the end. The study had few participants and a shorter intervention time. Schäffler et al. speculated that the temporary increase could either be because vitamin D only had a temporary effect on the bacterial communities, there is an optimal vitamin D level window, or that 4 weeks is too early to see long-term effects of vitamin D on the composition of the bacterial communities (55). In this thesis, there were more participants, 51 participants with 26 in placebo group and 25 in vitamin D group, with 2 months of intervention. An upregulation of butyrate in the form of TGs is observed. There is a possibility that with a larger study with more participants, increase in SCFA producing bacteria could also be seen in healthy subjects. It could also be speculated that 2 months of supplementation could be enough to see a long-term effect of vitamin D. Although, this would need to be further studied.

3 of the lipids contained 20:4, this could be the polyunsaturated fatty acid, arachidonic acid. In a study on maternal rats, rats receiving vitamin D deficient diet demonstrated higher arachidonic acid levels in both plasma and liver compared to controls which received a 1000 IU/kg diet. Therefore, indicating that maternal vitamin D deficiency may be associated with increased inflammation as arachidonic acid is known to produce proinflammatory mediators (56). The 3 lipids containing 20:4 all showed an increase in vitamin D group, though insignificantly. In this thesis, adipose tissue is investigated and not plasma or liver which could demonstrate a different outcome. A possible explanation could be that as an increased amount of 20:4 is found bound to TG, less is available to produce proinflammatory mediators and therefore reduce the inflammatory response. Nevertheless, as it is not known where the double bonds are located in the fatty acid, it could also possibly be the omega 3 isomer of eicosatetraenoic acid, which is a precursor of the omega 3 fatty acids eicosapentaenoic acid (20:5) and docosahexaenoic acid (22:6) which is known for exhibiting anti-inflammatory properties. Out of the 20 lipids in the data set one contains 20:5, also demonstrating an increase, though not significant. Though in the same study by Nandi et al. mentioned earlier, no change in plasma and liver omega 3 was observed, which could possibly be explained by compromised activity of desaturases in the omega 3 fatty acid metabolism pathway due to these desaturases being competitive and may be active in omega 6 metabolic pathway (56). If there is no competition from the omega 6 metabolic pathway with arachidonic acid, there could be a possibility of observing an increase in omega 3 fatty acids. Nonetheless, this is not certain and further studies is needed to examine the effect of vitamin D on eicosanoid metabolism and inflammation.

4.5 Other Analyses

In addition to the MVA, it was performed a pathway analysis, enrichment analysis, and a biomarker analysis on the 10 most important lipids for the OPLS model. The biomarker analysis was not able to identify any potential biomarkers among the 10 lipids. For the enrichment and pathway analysis, over half of the compounds IDs could not be matched to MetaboAnalyst's database. MetaboAnalyst obtained their lipids from the databases LIPID MAPS and RefMet but was not able to match all uploaded compound names to their internal compound database. The low identification rate may have caused the enrichment analysis to not show any noteworthy results.

Nevertheless, the pathway analysis was able to identify one pathway with more than one hit, the glycerophospholipid metabolism pathway, which was somehow different between placebo and vitamin D, despite the low identification rate. However, considering pathway impact and p-value in order to give an impression of the relevance of the findings, the influence of vitamin D on the glycerophospholipid metabolism pathway was not significant (p=0.901, impact factor=0,26). Out of the 36 compounds in the glycerophospholipid metabolism pathway, there were 4 that matched the dataset. These 4 were PE (C00350), PC (C00157), LPC (C04230), and PS (C02737), were LPC has the biggest impact. Within this pathway there is also LPE (C04438/C05973), which is also in the dataset but MetaboAnalyst was not able to identify and match with KEGG's pathway database.

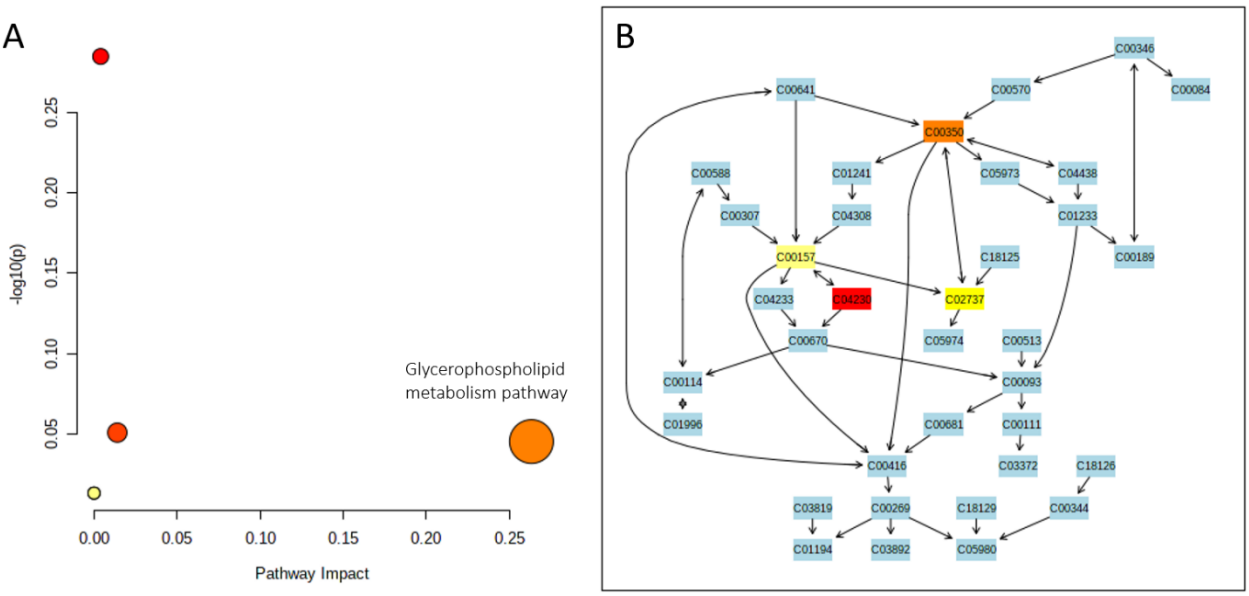

Figure 4-11 Result of pathway analysis. A: Overview of pathway analysis. B: Glycerophospholipid metabolism pathway.

4 of the 20 most influential lipids for the separation between the groups were lipids that are part of the glycerophospholipid metabolism pathway, PC 37:5e, PS 18:0 20:4, PE 40:8e and PC 20:4e 18:0, all of these having an increase after intervention with vitamin D. Though it's not significant, the pathway analysis showed a change in four metabolites of the glycerophospholipid metabolism, PE, PC, LPC and PS. In a cancer prevention study where baseline serum 25(OH)D and serum metabolites were measured in 392 men from 8 nested cancer case-control studies it was found that PE 18:0 20:4 and PE 18:0 18:2 were inversely related to serum 25(OH)D. Both glycerophospholipids were also inversely associated with aggressive prostate cancer risk (57). Though the role of vitamin D in cancer risk remains controversial, a case-cohort study showed no association between circulating 25(OH)D and prostate cancer (58). PE 18:0 20:4 was found in the dataset of this thesis. Even though it was not shown any significant increase or decrease in the vitamin D group in comparison to the placebo group, the lack of significance is most likely caused by large individual differences within the groups. In an untargeted clinical metabolomics study in humans, a significant reduction of PC after 4 weeks with 15 µg vitamin D daily was detected in the vitamin D responsive biomarker cluster characterized by low vitamin D status at baseline (<50 nmol/L) and higher plasma concentrations of resistin and adiponectin (59).

Vitamin D's connection to other components of the glycerophospholipid metabolism is established. A study reported that 1α,25$(OH)_2$D caused a 61% increase in glycerol-3-phosphate dehydrogenase (GPDH) activity in human adipocytes, while 1β,25$(OH)_2$D inhibited this effect (60). GPDH is an important enzyme of intermediary metabolism and a component of glycerophosphate shuttle where it connects glycolysis, oxidative phosphorylation, and fatty acid metabolism together (61).

5 Conclusion

A sample preparation method to simultaneously extract lipid and metabolites from adipose tissue for analysis with UHPLC-MS was developed and tested for both lipids and metabolites. Lipid fractions of 102 samples were analyzes by UPLC-MS and data processed, while the metabolite fractions are stored at -80ºC awaiting instrument method development and validation prior to analysis.

The result of the multivariate data analysis did not show any separation between vitamin D and placebo group in PCA, but showed separation when applying the supervised discriminant analysis, OPLS. The OPLS demonstrated that the lipidome in adipose tissue correlates to 25(OH)D in serum to a greater degree than vitamin D in the adipose tissue. This could indicate that the composition of lipids in the adipose tissue is due to vitamin D's activity not in the adipose tissue, but other parts of the body such as the liver.

Out of the 20 most important lipids that caused the separation between the groups only 2 showed a significant difference between vitamin D and placebo group. 6 out of the 20 contained the short-chain fatty acid butyrate, produced in the intestinal lumen, which could further indicate that vitamin D executes its activity outside of the adipose tissue. 4 of the 20 lipids contained either 20:4 or 20:5 fatty acids, which could indicate an effect of vitamin D on the eicosanoid metabolism.

The pathway analysis was able to identify the glycerophospholipid metabolism pathway in which there was found a difference between vitamin D and placebo group, although it was unfortunately not statistically significant.

References

1. Sniadecki SJJ, Sniadecki J. on the cure of rickets.(1840) Cited by W. Mozolowski. Nature. 1939;143:121-4.
2. Palm TA. The geographical distribution and aetiology of rickets. Practitioner. 1890;45(270-9):106-63.
3. Holick MF. Sunlight and vitamin D for bone health and prevention of autoimmune diseases, cancers, and cardiovascular disease. Am J Clin Nutr. 2004;80(6):1678S-88S.
4. Loomis WF. Rickets. Sci Am. 1970;223(6):76-82 passim.
5. Weick MT. A history of rickets in the United States. Am J Clin Nutr. 1967;20(11):1234-41.
6. DeLuca HF. Overview of general physiologic features and functions of vitamin D. Am J Clin Nutr. 2004;80(6):1689S-96S.
7. Hossein-nezhad A, Holick MF. Vitamin D for Health: A Global Perspective. Mayo Clin Proc. 2013;88(7):720-55.
8. Chun RF. New perspectives on the vitamin D binding protein. Cell Biochem Funct. 2012;30(6):445-56.
9. Carlberg C. The physiology of vitamin D - far more than calcium and bone. Front Physiol. 2014;5:335-.
10. Seamans KM, Cashman KD. Existing and potentially novel functional markers of vitamin D status: A systematic review. Am J Clin Nutr. 2009;89(6):1997S-2008S.
11. Misra M, Pacaud D, Petryk A, Collett-Solberg PF, Kappy M. Vitamin D Deficiency in Children and Its Management: Review of Current Knowledge and Recommendations. Pediatrics. 2008;122(2):398-417.
12. Holick MF. Vitamin D and Health: Evolution, Biologic Functions, and Recommended Dietary Intakes for Vitamin D. In: Holick MF, editor. Vitamin D: Physiology, Molecular Biology, and Clinical Applications. Totowa, NJ: Humana Press; 2010. p. 3-33.
13. Holick MF. Vitamin D: importance in the prevention of cancers, type 1 diabetes, heart disease, and osteoporosis. Am J Clin Nutr. 2004;79(3):362-71.
14. Bendik I, Friedel A, Roos FF, Weber P, Eggersdorfer M. Vitamin D: a critical and essential micronutrient for human health. Front Physiol. 2014;5:248-.
15. Bischoff-Ferrari HA, Giovannucci E, Willett WC, Dietrich T, Dawson-Hughes B. Estimation of optimal serum concentrations of 25-hydroxyvitamin D for multiple health outcomes. Am J Clin Nutr. 2006;84(1):18-28.
16. IOM. Dietary Reference Intakes for Calcium and Vitamin D. Washington, D.C: Institute of Medicine. National Academies Press; 2011.
17. Meyer H, Nasjonalt råd for e. Tiltak for å sikre en god vitamin D-status i befolkningen : rapport fra en arbeidsgruppe nedsatt av Nasjonalt råd for ernæring. Oslo: Nasjonalt råd for ernæring; 2006.
18. Helsedirektoratet. Norwegian guidelines on diet, nutrition and physical activity: Norwegian Directorate of Health; 2020.
19. Ahima RS. Adipose Tissue as an Endocrine Organ. Obesity (Silver Spring). 2006;14(S8):242S-9S.
20. Choe SS, Huh JY, Hwang IJ, Kim JI, Kim JB. Adipose Tissue Remodeling: Its Role in Energy Metabolism and Metabolic Disorders. Front Endocrinol (Lausanne). 2016;7:30-.
21. Abbas MA. Physiological functions of Vitamin D in adipose tissue. J Steroid Biochem Mol Biol. 2017;165(Pt B):369-81.
22. Rosenstreich SJ, Rich C, Volwiler W. Deposition in and release of vitamin D3 from body fat: evidence for a storage site in the rat. J Clin Invest. 1971;50(3):679-87.

23. Didriksen A, Burild A, Jakobsen J, Fuskevåg OM, Jorde R. Vitamin D3 increases in abdominal subcutaneous fat tissue after supplementation with vitamin D3. Eur J Endocrinol. 2015;172(3):235-41.
24. Wortsman J, Matsuoka LY, Chen TC, Lu Z, Holick MF. Decreased bioavailability of vitamin D in obesity. Am J Clin Nutr. 2000;72(3):690-3.
25. Ding C, Gao D, Wilding J, Trayhurn P, Bing C. Vitamin D signalling in adipose tissue. Br J Nutr. 2012;108(11):1915-23.
26. Hasin Y, Seldin M, Lusis A. Multi-omics approaches to disease. Genome Biol. 2017;18(1):83-15.
27. Debnath M, Prasad G, Bisen P. Molecular Diagnostics : Promises and Possibilities2010.
28. Wishart DS. Metabolomics for Investigating Physiological and Pathophysiological Processes. Physiological Reviews. 2019;99(4):1819-75.
29. Zhang A, Sun H, Wang P, Han Y, Wang X. Modern analytical techniques in metabolomics analysis. Analyst. 2012;137(2):293-300.
30. Züllig T, Trötzmüller M, Köfeler HC. Lipidomics from sample preparation to data analysis: a primer. Anal Bioanal Chem. 2020;412(10):2191-209.
31. Holčapek M, Liebisch G, Ekroos K. Lipidomic Analysis. Anal Chem. 2018;90(7):4249-57.
32. LIPID MAPS 2020 [cited 2020 November]. Available from: www.lipidmaps.org.
33. Shevchenko A, Simons K. Lipidomics: coming to grips with lipid diversity. Nat Rev Mol Cell Biol. 2010;11(8):593-8.
34. Roškar R. Analytical Methods for Quantification of Drug Metabolites in Biological Samples. IntechOpen; 2012, p.100-102.
35. Berk Z. Food Process Engineering and Technology. San Diego: San Diego: Elsevier Science & Technology; 2013, p.259-260, p.276-277.
36. Pedersen-Bjergaard S, Gammelgaard B, Halvorsen TG. Introduction to pharmaceutical analytical chemistry. Hoboken, NJ: Wiley; 2019, p. 185-191, p.231-258.
37. Moldoveanu SC, David V. Essentials in Modern HPLC Separations. Saint Louis: Saint Louis: Elsevier; 2012, p.1-14.
38. Kaufmann A. Analytical performance of the various acquisition modes in Orbitrap MS and MS/MS. J Mass Spectrom. 2018;53(8):725-38.
39. Mutch DM, Tordjman J, Pelloux V, Hanczar B, Henegar C, Poitou C, et al. Needle and surgical biopsy techniques differentially affect adipose tissue gene expression profiles. The American Journal of Clinical Nutrition. 2008;89(1):51-7.
40. Matyash V, Liebisch G, Kurzchalia TV, Shevchenko A, Schwudke D. Lipid extraction by methyl- tert -butyl ether for high-throughput lipidomics. J Lipid Res. 2008;49(5):1137-46.
41. Coman C, Solari FA, Hentschel A, Sickmann A, Zahedi RP, Ahrends R. Simultaneous metabolite, protein, lipid extraction (SIMPLEX): A combinatorial multimolecular omics approach for systems biology. Mol Cell Proteomics. 2016;15(4):1453-66.
42. ThermoFisher. LipidSearch™ Software 2021 [cited 2021 09.04]. Available from: https://www.thermofisher.com/order/catalog/product/IQLAAEGABSFAPCMBFK#/IQLAAEGABSFAPCMBFK.
43. Sartorius. MVDA Software Provides Insights into Your Process Data: Sartorius; 2021 [Available from: https://www.sartorius.com/en/products/process-analytical-technology/data-analytics-software/mvda-software.
44. MetaboAnalyst. MetaboAnalyst5.0 - user-friendly, streamlined metabolomics data analysis 2021 [cited 2021 09.04]. Available from: https://www.metaboanalyst.ca/home.xhtml.
45. Bligh EG, Dyer WJ. A rapid method of total lipid extraction and purification. Can J Biochem Physiol. 1959;37(8):911-7.

46. Sostare J, Di Guida R, Kirwan J, Chalal K, Palmer E, Dunn WB, et al. Comparison of modified Matyash method to conventional solvent systems for polar metabolite and lipid extractions. Anal Chim Acta. 2018;1037:301-15.
47. Worley B, Powers R. Multivariate Analysis in Metabolomics. Curr Metabolomics. 2013;1(1):92-107.
48. Esposito Vinzi V, Chin WW, Henseler J, Wang H. Handbook of Partial Least Squares : Concepts, Methods and Applications. Berlin, Heidelberg: Springer Berlin Heidelberg : Imprint: Springer; 2010.
49. Asano L, Watanabe M, Ryoden Y, Usuda K, Yamaguchi T, Khambu B, et al. Vitamin D Metabolite, 25-Hydroxyvitamin D, Regulates Lipid Metabolism by Inducing Degradation of SREBP/SCAP. Cell Chem Biol. 2017;24(2):207-17.
50. Best CM, Riley DV, Laha TJ, Pflaum H, Zelnick LR, Hsu S, et al. Vitamin D in human serum and adipose tissue after supplementation. Am J Clin Nutr. 2020.
51. Martinaityte I, Kamycheva E, Didriksen A, Jakobsen J, Jorde R. Vitamin D Stored in Fat Tissue During a 5-Year Intervention Affects Serum 25-Hydroxyvitamin D Levels the Following Year. J Clin Endocrinol Metab. 2017;102(10):3731-8.
52. Hengist A, Perkin O, Gonzalez JT, Betts JA, Hewison M, Manolopoulos KN, et al. Mobilising vitamin D from adipose tissue: The potential impact of exercise. Nutrition bulletin. 2019;44(1):25-35.
53. Liu H, Wang J, He T, Becker S, Zhang G, Li D, et al. Butyrate: A Double-Edged Sword for Health? Adv Nutr. 2018;9(1):21-9.
54. Battistini C, Ballan R, Herkenhoff ME, Saad SMI, Sun J. Vitamin D Modulates Intestinal Microbiota in Inflammatory Bowel Diseases. Int J Mol Sci. 2021;22(1):362.
55. Schäffler H, Herlemann DPR, Klinitzke P, Berlin P, Kreikemeyer B, Jaster R, et al. Vitamin D administration leads to a shift of the intestinal bacterial composition in Crohn's disease patients, but not in healthy controls. J Dig Dis. 2018;19(4):225-34.
56. Nandi A, Wadhwani N, Joshi SR. Vitamin D deficiency influences fatty acid metabolism. Prostaglandins Leukot Essent Fatty Acids. 2019;140:57-63.
57. Nelson SM, Panagiotou OA, Anic GM, Mondul AM, Mannisto S, Weinstein SJ, et al. Metabolomics analysis of serum 25-hydroxy-vitamin D in the Alpha-Tocopherol, Beta-Carotene Cancer Prevention (ATBC) Study. Int J Epidemiol. 2016;45(5):1458-68.
58. Heath AK, Hodge AM, Ebeling PR, Eyles DW, Kvaskoff D, Buchanan DD, et al. Circulating 25-Hydroxyvitamin D Concentration and Risk of Breast, Prostate, and Colorectal Cancers: The Melbourne Collaborative Cohort Study. Cancer Epidemiol Biomarkers Prev. 2019;28(5):900-8.
59. O'Sullivan A, Gibney MJ, Connor AO, Mion B, Kaluskar S, Cashman KD, et al. Biochemical and metabolomic phenotyping in the identification of a vitamin D responsive metabotype for markers of the metabolic syndrome. Mol Nutr Food Res. 2011;55(5):679-90.
60. Shi H, Norman AW, Okamura WH, Sen A, Zemel MB. 1α,25-Dihydroxyvitamin D3 modulates human adipocyte metabolism via nongenomic action. The FASEB journal. 2001;15(14):1-15.
61. Mráček T, Drahota Z, Houštěk J. The function and the role of the mitochondrial glycerol-3-phosphate dehydrogenase in mammalian tissues. Biochimica et biophysica acta Bioenergetics. 2013;1827(3):401-10.

Appendix

Appendix 1: Samples

#	Study	ID	Visit	Treatment	Serum $25(OH)_2D$ (nmol/L)	Fat vitamin D (ng/g)
1	Global 1	1026	Baseline	Placebo	41	18
2	Global 1		Endpoint	Placebo	23.6	15
3	Global 1	1035	Baseline	Vitamin D	39	4.2
4	Global 1		Endpoint	Vitamin D	114.6	47
5	Global 1	1041	Baseline	Vitamin D	40	24
6	Global 1		Endpoint	Vitamin D	101.9	53
7	Global 1	1052	Baseline	Vitamin D	42	16
8	Global 1		Endpoint	Vitamin D	86.4	83
9	Global 1	1055	Baseline	Vitamin D	39	22
10	Global 1		Endpoint	Vitamin D	139.2	50
11	Global 1	1063	Baseline	Placebo	24	3.3
12	Global 1		Endpoint	Placebo	11.3	2.5
13	Global 1	1072	Baseline	Vitamin D	45	69
14	Global 1		Endpoint	Vitamin D	77.5	95
15	Global 1	1081	Baseline	Placebo	33	5.2
16	Global 1		Endpoint	Placebo	18	4
17	Global 1	1091	Baseline	Vitamin D	26	25
18	Global 1		Endpoint	Vitamin D	86.4	56
19	Global 1	1096	Baseline	Vitamin D	36	9.4
20	Global 1		Endpoint	Vitamin D	149.1	49
21	Global 1	1098	Baseline	Placebo	38	22
22	Global 1		Endpoint	Placebo	20.4	18
23	Global 1	1177	Baseline	Vitamin D	43	36
24	Global 1		Endpoint	Vitamin D	91.7	104
25	Global 1	1186	Baseline	Placebo	38	11.6
26	Global 1		Endpoint	Placebo	26.1	10.9
27	Global 1	1187	Baseline	Placebo	45	20
28	Global 1		Endpoint	Placebo	21.3	19
29	Global 1	1188	Baseline	Placebo	42	8.8
30	Global 1		Endpoint	Placebo	27.9	9.2

31	Global 1	1189	Baseline	Placebo	36	5.6
32	Global 1		Endpoint	Placebo	21.3	5.6
33	Global 1	1200	Baseline	Placebo	42	35
34	Global 1		Endpoint	Placebo	22	34
35	Global 1	1214	Baseline	Vitamin D	35	36
36	Global 1		Endpoint	Vitamin D	84	79
37	Global 1	1228	Baseline	Placebo	40	13.9
38	Global 1		Endpoint	Placebo	28	17
39	Global 2	5715	Baseline	Placebo	38.8	104
40	Global 2		Endpoint	Placebo	38.2	108
41	Global 2	5716	Baseline	Placebo	38.4	18
42	Global 2		Endpoint	Placebo	30.6	19
43	Global 2	5717	Baseline	Placebo	46.8	23
44	Global 2		Endpoint	Placebo	39.4	23
45	Global 2	5718	Baseline	Vitamin D	29.9	8
46	Global 2		Endpoint	Vitamin D	96.1	67
47	Global 2	5719	Baseline	Vitamin D	32.9	-
48	Global 2		Endpoint	Vitamin D	89.5	37
49	Global 2	5720	Baseline	Placebo	26.5	8.4
50	Global 2		Endpoint	Placebo	23.8	8.2
51	Global 2	5721	Baseline	Vitamin D	45.8	-
52	Global 2		Endpoint	Vitamin D	86.5	106
53	Global 2	5722	Baseline	Vitamin D	37.2	26
54	Global 2		Endpoint	Vitamin D	83.4	66
55	Global 2	5723	Baseline	Placebo	27.4	4.5
56	Global 2		Endpoint	Placebo	27.8	6.1
57	Global 2	5724	Baseline	Vitamin D	28.3	13
58	Global 2		Endpoint	Vitamin D	86.5	35
59	Global 2	5725	Baseline	Placebo	24.1	18
60	Global 2		Endpoint	Placebo	23.2	19
61	Global 2	5726	Baseline	Vitamin D	24.7	38
62	Global 2		Endpoint	Vitamin D	92.8	56
63	Global 2	5727	Baseline	Placebo	33.5	15
64	Global 2		Endpoint	Placebo	24.5	10.9
65	Global 2	5728	Baseline	Vitamin D	43.9	81

66	Global 2		Endpoint	Vitamin D	73.7	105
67	Global 2	5729	Baseline	Vitamin D	28.1	33
68	Global 2		Endpoint	Vitamin D	99.8	113
69	Global 2	5730	Baseline	Placebo	26.1	10.1
70	Global 2		Endpoint	Placebo	27.1	7
71	Global 2	5731	Baseline	Placebo	30.8	12
72	Global 2		Endpoint	Placebo	35.5	11.4
73	Global 2	5732	Baseline	Vitamin D	35.5	26
74	Global 2		Endpoint	Vitamin D	103.6	86
75	Global 2	5733	Baseline	Placebo	39.7	11
76	Global 2		Endpoint	Placebo	25.7	8.7
77	Global 2	5734	Baseline	Placebo	27.4	19
78	Global 2		Endpoint	Placebo	29.8	19
79	Global 2	5735	Baseline	Vitamin D	30.2	9.1
80	Global 2		Endpoint	Vitamin D	112.6	75
81	Global 2	5736	Baseline	Vitamin D	38.1	17
82	Global 2		Endpoint	Vitamin D	120.5	54
83	Global 2	5737	Baseline	Placebo	37.7	16
84	Global 2		Endpoint	Placebo	29.6	19
85	Global 2	5738	Baseline	Placebo	35.9	24
86	Global 2		Endpoint	Placebo	35.5	18
87	Global 2	5739	Baseline	Vitamin D	27	15
88	Global 2		Endpoint	Vitamin D	92.8	43
89	Global 2	5740	Baseline	Vitamin D	33.1	6.6
90	Global 2		Endpoint	Vitamin D	105.8	44
91	Global 2	5741	Baseline	Placebo	40.7	54
92	Global 2		Endpoint	Placebo	37.1	60
93	Global 2	5742	Baseline	Placebo	37.2	27
94	Global 2		Endpoint	Placebo	29.3	18
95	Global 2	5743	Baseline	Vitamin D	39.9	28
96	Global 2		Endpoint	Vitamin D	118.7	138
97	Global 2	5744	Baseline	Placebo	40.2	33
98	Global 2		Endpoint	Placebo	35.8	48
99	Global 2	5747	Baseline	Vitamin D	26.7	12.1
100	Global 2		Endpoint	Vitamin D	108	67

101	Global 2	5748	Baseline	Vitamin D	35.2	23
102	Global 2		Endpoint	Vitamin D	93.7	89

-: Missing, sample was lost during the analysis

Appendix 2: Instrument Settings

Table 1 Full list of Orbitrap IdX™ Tribrid™ settings for the analysis of the lipidome

Ion source	
Ion source type	H-ESI
Spray voltage	Static
Positive/Negative ion (V)	3500/2500
Sheath gas (arb)	60
Aux gas (arb)	15
Sweep gas (arb)	2
Ion transfer tube temperature (ºC)	350
Vaporizer temperature (ºC)	350
MS Global settings	
Method Duration (min)	30
Infusion mode	Liquid chromatography
Expected LC peak width (s)	3
Internal mass calibration	Easy-IC
Data dependent mode	Cycle time
Cycle time (s)	1.5
MS OT	
Orbitrap resolution	120 000
Use quadrupole isolation	True
Scan range (m/z)	250-1500
RF lens (%)	40
AGC target	400 000
Maximum injection time (ms)	50
Polarity	Positive
Source fragmentation	Disabled
Use EASY-IC	True
Intensity filter	
Minimum intensity	25 000
Maximum intensity	1E+20
Dynamic exclusion	
Exclude after n times	1
Exclusion duration (s)	2
Exclude isotopes	True
ddMS2 OT HCD	
Isolation mode	Quadrupole
Isolation window (m/z)	1.5
Activation type	HCD
Collision energy mode	Stepped

Collision energies (%)	25, 30, 35
Orbitrap resolution	15 000
Scan range mode	Define first mass
First mass (m/z)	140
Maximum injection time (ms)	50
AGC target	50 000
Microscans	1
Use EASY-IC	True
ddMS2 OT CID	
Scan priority	1
Isolation mode	Quadrupole
Isolation window (m/z)	2
Activation type	CID
Collision energy mode	Fixed
Collision energy (%)	32
CID activation time (ms)	10
Orbitrap resolution	15 000
Scan range mode	Auto
Maximum injection time (ms)	50
AGC target	50 000
Microscans	1
Use EASY-IC	False
Number of dependent scans	1
ddMS3 OT	
Scan priority	1
Isolation window	1.5
MS2 isolation window	2.2
Activation type	CID
Collision energy mode	Fixed
Collision energy (%)	35
Activation time (ms)	10
Activation Q	0.25
Orbitrap resolution	15 000
Scan range mode	Auto
Maximum injection time (ms)	65
AGC target	50 000
Microscans	1
Use EASY-IC	False
Number of dependent scans	3

Table 2 Full list of Orbitrap IdX™ Tribrid™ settings for the analysis of the metabolome

Ion source	**Positive**	**Negative**
Ion source type	H-ESI	H-ESI
Spray voltage	Static	Static
Positive/Negative ion (V)	3500/2500	3500/2500
Sheath gas (arb)	50	50
Aux gas (arb)	10	10
Sweep gas (arb)	0	0
Ion transfer tube temperature	325	325
Vaporizer temperature (ºC)	350	350
MS Global settings		
Method Duration (min)	16	15
Infusion mode	Liquid chromatography	Liquid chromatography
Expected LC peak width (s)	3	3
Internal mass calibration	Easy-IC	Easy-IC
Data dependent mode	Cycle time	Cycle time
Cycle time (s)	0.6	0.6
MS OT		
Orbitrap resolution	60 000	60 000
Use quadrupole isolation	True	True
Scan range (m/z)	70-800	70-800
RF lens (%)	35	35
AGC target	100 000	100 000
Maximum injection time (ms)	50	50
Polarity	Positive	Negative
Source fragmentation	Disabled	Disabled
Use EASY-IC	True	True
Intensity filter		
Minimum intensity	20 000	20 000
Maximum intensity	1E+20	1E+20
Dynamic exclusion		
Exclude after n times	1	1
Exclusion duration (s)	2.5	2.5
Exclude isotopes	True	True
ddMS2 OT HCD		
Isolation mode	Quadrupole	Quadrupole
Isolation window (m/z)	1.5	1.5
Activation type	HCD	HCD
Collision energy mode	Stepped	Stepped
Collision energies (%)	20, 35, 50	20, 35, 50

Orbitrap resolution	30 000	30 000
Scan range mode	Auto	Auto
Maximum injection time (ms)	54	54
AGC target	50 000	50 000
Microscans	1	1
Use EASY-IC	False	False